HOKKAIDO UNIVERSITY

Title	Conditioned medium from human amnion-derived mesenchymal stem cells regulates activation of primary hepatic stellate cells
Author(s)	付, 慶傑
Citation	北海道大学. 博士(医学) 甲第14093号
Issue Date	2020-03-25
DOI	10.14943/doctoral.k14093
Doc URL	http://hdl.handle.net/2115/77929
Type	theses (doctoral)
Note	配架番号：2559
File Information	Fu_Qingjie.pdf

Instructions for use

Hokkaido University Collection of Scholarly and Academic Papers : HUSCAP

学　位　論　文

Conditioned medium from human amnion-derived mesenchymal stem cells regulates activation of primary hepatic stellate cells

(羊膜間葉系幹細胞由来培養上清の培養肝星細胞に対する活性化制御)

2020 年 3 月
北 海 道 大 学

付 慶傑
Fu Qingjie

学　位　論　文

Conditioned medium from human amnion-derived mesenchymal stem cells regulates activation of primary hepatic stellate cells

(羊膜間葉系幹細胞由来培養上清の培養肝星細胞に対する活性化制御)

2020 年 3 月
北 海 道 大 学

付 慶傑
Fu Qingjie

Table of contents

LIST OF PUBLICATIONS AND PRESENTATIONS

Publications

1. Fu Q., Ohnishi S., Sakamoto N. “Conditioned medium from human amnion-derived mesenchymal stem cells regulates activation of primary hepatic stellate cells,” Stem Cells International 2018;2018:4898152.

2. Ohara M., Ohnishi S., Hosono H., Yamamoto K., Fu Q., Maehara O., Suda G and Sakamoto N. “Palmitoylethanolamide ameliorates carbon tetrachloride-induced liver fibrosis in rats,” Front. Pharmacol 2018;9:709.

3. Ohara M., Ohnishi S., Hosono H., Yamamoto K., Yuyama K., Nakamura H., Fu Q., Maehara O., Suda G and Sakamoto N. “Extracellular vesicles from amnion-derived mesenchymal stem cells ameliorate hepatic inflammation and fibrosis in rats,” Stem Cells International 2018;2018:3212643.

Presentations

Fu Q., Ohnishi S., Sakamoto N. “Conditioned medium from human amnion-derived mesenchymal stem cells regulated activation of primary hepatic stellate cells,” The 18th Congress of the Japanese Society for Regenerative Medicine, Kobe, Japan, March 21-23, 2019 (Poster).

ABSTRACT

Background and Aim: Mesenchymal stem cells (MSCs) are stromal cells that exhibit the ability of multilineage differentiation and possess the capacity to self-renew, and reside in almost all organs and tissues. Although MSCs were first reported to be derived from bone marrow, they have been isolated from almost all tissues including adipose tissue, umbilical cord, amnion and dental pulp. Because of advantages that human amnion mesenchymal stem cells (hAMSCs) can be obtained in large amount without invasive procedures and are with enormous proliferative capacity, it has attracted much attention in the fields of cell therapy and regenerative medicine. Researchers have widely demonstrated the anti-inflammatory, anti-fibrotic and anti-apoptotic effects of MSCs in either MSC transplantation or application of conditioned medium obtained from MSCs, and hAMSC transplantation has been reported to ameliorate liver fibrosis in animal models. Hepatic stellate cells (HSCs) are the key contributors to liver fibrogenesis, and following liver injury, HSCs undergo activation which means a transition from quiescent vitamin A-rich cells into proliferative, fibrogenic, and contractile myofibroblasts. As the mechanism by which hAMSCs prevent liver fibrosis is poorly understood, I investigated if conditioned medium from hAMSC cultures (hAMSC-CM) inhibit HSCs activation *in vitro*.

Methods and Results: My experiment mainly consisted of two parts. The first part was the isolation of rat HSCs, and the second part was to explore the effect of hAMSC-CM on primary HSCs. In order to obtain high-purity HSCs, fluorescence-activated cell sorting (FACS) was performed depending on the autofluorescence in primary HSCs, followed by density gradient centrifugation. The sorted cells showed high expression of platelet-derived growth factor receptor beta (*Pdgfrb*) expression, and low expression of C-type lectin domain family 4f (*Clec4f*), and *albumin*, which means that HSCs were efficiently purified but Kupffer cells and hepatocytes were rarely included in the sorted cells. Moreover, the flow cytometry results showed that the sorted cells had high expression of desmin with the rate of 74.6 %, but no expression of CD31 (endothelial cells) and CD163 (Kupffer cells). Furthermore, retinol-based autofluorescence was used to confirm the purity of sorted HSCs, exhibiting a final purity of > 98%. The freshly isolated HSCs were irregularly round shaped, and their cytoplasm was rich in lipid droplets. When excited at 352 nm LASER, the vitamin A–rich lipid droplets emitted blue autofluorescence. Post-culturing for 2 days, HSCs became extended and presented an asteroid phenotype, accompanied by a reduction of lipid droplets. HSCs were further activated by routine culture, and it was difficult to observe autofluorescence post-culturing for 4 days, suggesting that quiescent HSCs were activated by

routine culture. Isolated HSCs proliferated well after seeding and long-term culture showed that HSCs proliferated rapidly with good viability. These results fully demonstrated that I obtained HSCs with high purity and activity, and the sorted HSCs could be applied for further experiments. After isolating HSCs, I cultured HSCs in hAMSC-CM or standard medium (SM) to investigate the effect of hAMSC-CM on HSC activation in routine culture. I found that hAMSC-CM inhibited the expression of α smooth muscle actin (α-SMA) both at gene level and protein level. Moreover, the expression of matrix metalloproteinases (*Mmps*) including *Mmp2*, *Mmp9*, and *Mmp13* was markedly increased by hAMSC-CM, but hAMSC-CM did not affect the synthesis of collagen type I α1 (*Col1a1*). Even though the expression of tissue inhibitor of metalloproteinase 1 (*Timp1*) was also up-regulated by hAMSC-CM, the extracellular matrix (ECM)-associated genes were down-regulated by hAMSC-CM, which was evaluated by the ratio of *Mmp13/Timp1*, and the interstitial collagen I which was measured by ELISA was decreased as well. In addition, I also found that the inhibitory effect of hAMSC-CM on HSC activation was concentration-dependent. Next, I examined if hAMSC-CM affect proliferation of HSCs. Gene expression of G2/M-associated proteins such as cyclin B1 (*Ccnb-1*) and B2 (*Ccnb-2*) were inhibited by hAMSC-CM, and cell proliferation assay using CCK-8 also showed that HSC proliferation was inhibited in culture with hAMSC-CM. Besides routine culture, I cultured HSCs with transforming growth factor-β (TGFβ), the most efficient collagen synthesis factor, to investigate whether hAMSC-CM antagonize the pro-fibrogenic effect of TGFβ. As a result, hAMSC-CM reduced the gene expression of *α-Sma* promoted by TGFβ, indicating that hAMSC-CM inhibited TGFβ-induced HSC activation. Although hAMSC-CM did not affect the expression of *Col1a1* in routine culture, the up-regulated expression of *Col1a1* induced by TGFβ was significantly suppressed by hAMSC-CM. Along with up-regulation of *Col1a1*, TGFβ inhibited expression of *Mmps* to promote ECM accumulation. hAMSC-CM remitted this inhibition and significantly increased the expression of *Mmps*. The ratio of *Mmp13/Timp1* was obviously upgraded by hAMSC-CM as well, which implied that hAMSC-CM promoted ECM degradation even in the presence of TGFβ. Overall, hAMSC-CM exhibited the capacity of inhibiting the accumulation of ECM at gene expression level. Interestingly, the gene expression of TGFβ receptor 1 (*Tgfbr1*) was increased more by hAMSC-CM than by TGFβ. Furthermore, given that hAMSCs are likely to be contaminated with fibroblasts by using current isolation scheme and in order to investigate whether the suppressive effect on HSCs is specific to hAMCS-CM, I cultured HSCs with conditioned medium obtained from skin fibroblasts (fibroblast-CM). Although fibroblast-CM significantly enhanced *Col1a1*

expression and suppressed *Timp-2* expression in HSCs, it increased the expression of *Mmps* and *Timp-1*, and decreased the expression of *α-Sma* and *Ccnbs* as well.

Discussion: In the present study, I obtained highly purified HSCs and I demonstrated the anti-activation effect of hAMSC-CM on HSCs *in vitro*. Followed by density gradient centrifugation, additional autofluorescence-based FACS greatly improved the purity of HSCs. Moreover, given the specificity of HSC markers is still questionable, in order to accurately confirm the purity of isolated HSCs, autofluorescence was used instead of using those markers. α-SMA is the activation marker of HSC, and the decreased α-SMA expression at both gene and protein levels indicated HSC activation was inhibited by hAMSC-CM. When HSCs are activated, large amounts of COL1 are secreted, leading excessive ECM accumulation. In this study, I showed that hAMSC-CM decreases COL1 accumulation. On the basis of that hAMSC-CM does not influence *Col1a1* expression but has a positive effect on *Mmps* and *Timps*, I believe that instead of inhibiting COL1 synthesis in routine culture of HSCs, hAMSC-CM reduces ECM accumulation by promoting COL1 degradation. HSC activation is accompanied by massive cell proliferation, and proliferation assay indicated that hAMSC-CM reduces HSC proliferation in this study. Inhibited expression of *Ccnbs* suggested that this process is performed by regulating the cell cycle. TGFβ is the most efficient fibrogenic factor and HSCs can be activated further by TGFβ. In this study, I observed that hAMSC-CM inhibits TGFβ1-induced HSC activation. In addition, I found that hAMSC-CM contains TGFβ1, and hAMSC-CM induced *Tgfbr1* up-regulation is most likely caused by additional exogenous TGFβ1. The similar effects shown by hAMSC-CM and fibroblast-CM suggest that hAMSCs and fibroblasts have something in common in certain functions, but their common mechanism is unclear.

Conclusions: The major findings in my study were (1) hAMSC-CM inhibited the activation of HSCs, (2) hAMSC-CM regulated the accumulation of ECM during the activation of HSCs, (3) hAMSC-CM suppressed the proliferation of HSCs. These findings demonstrate that hAMSC-CM can modulate the function of HSCs via secretory factors and provide a plausible explanation for the protective role of hAMSCs in liver fibrosis.

LIST OF ABBREVIATIONS

18S rRNA	18S ribosomal ribonucleic acid
7-AAD	7-aminoactinomycin D solution
α-SMA	Alpha–smooth muscle actin
ANOVA	Analysis of variance
APC	Allophycocyanin
BM-MSC	Bone marrow-derived mesenchymal stem cell
BSA	Bovine serum albumin
CCK-8	Cell Counting Kit-8
CCNB-1	Cyclin B1
CCNB-2	Cyclin B2
CD11b	Cluster of differentiation 11b
CD19	Cluster of differentiation 19
CD26	Cluster of differentiation 26
CD31	Cluster of differentiation 31
CD34	Cluster of differentiation 34
CD38	Cluster of differentiation 38
CD44	Cluster of differentiation 44
CD45	Cluster of differentiation 45
CD73	Cluster of differentiation 73
CD90	Cluster of differentiation 90
CD105	Cluster of differentiation 105
CD163	Cluster of differentiation 163
cDNA	Complementary deoxyribonucleic acid
CLEC4F	C-type lectin domain family 4f
CO2	Carbon dioxide
COL1	Collagen type 1
COL1A1	Collagen type 1 alpha 1
DMEM	Dulbecco minimal essential medium
DNase I	Deoxyribonuclease I
ECM	Extracellular matrix
EDTA	Ethylenediaminetetraacetic acid
ELISA	Enzyme-linked immunosorbent assay

EtOH	Ethanol
FACS	Fluorescence-activated cell sorting
FBS	Fetal bovine serum
Fibroblast-CM	Conditioned medium obtained from skin fibroblast cultures
FITC	Fluorescein-isothiocyanate
FSC	Forward scatter
FSC-A	Forward scatter area
FSC-H	Forward scatter height
gDNA	Genomic deoxyribonucleic acid
GFAP	Glial fibrillary acidic protein
hAMSC	Human amnion-derived mesenchymal stem cell
hAMSC-CM	Conditioned medium obtained from human amnion-derived mesenchymal stem cell cultures
HBSS (–)	Hank's-balanced salt solution without calcium, magnesium, or phenol red
HBSS (+)	Hank's-balanced salt solution with calcium, magnesium, but without phenol red
HCC	Hepatocellular carcinoma
HCL	Hydrogen chloride
HEPES	4-(2-hydroxyethyl)-1-piperazineethanesulfonic acid
HLA-DR	Human leukocyte antigen–antigen DR
HSC	Hepatic stellate cell
IL-10	Interleukin 10
ITGA11	Integrin alpha 11
IVC	Inferior vena cava
Mean ± SD	Mean ± standard deviation
MEMα	Minimum essential medium alpha
MeOH	Methanol
MMP-2	Metalloproteinase-2
MMP-9	Metalloproteinase-9
MMP-13	Metalloproteinase-13
MSC	Mesenchymal stem cell
NaCl	Sodium chloride
NaOH	Sodium hydroxide

PBS	Phosphate buffered saline
PCR	Polymerase chain reaction
PDGF	Platelet-derived growth factor
PDGFRβ	Platelet-derived growth factor receptor beta
PE	Phycoerythrin
qRT-PCR	Quantitative reverse-transcription polymerase chain reaction
RNA	Ribonucleic acid
SD rat	Sprague–Dawley rat
SM	Standard medium
SSC	Sideward scatter
SteCGS	Stellate cell growth supplement
SteCM	Stellate cell medium
TGFβ	Transforming growth factor–beta
TGFβR1	TGFβ receptor 1
TIMP-1	Tissue inhibitor of metalloproteinase-1
TIMP-2	Tissue inhibitor of metalloproteinase-2
TNF-α	Tumor necrosis factor alpha

INTRODUCTION

1. Liver fibrosis and cirrhosis

Chronic liver diseases are characterized by a prolonged wound healing response, which frequently move forward to advanced fibrosis and cirrhosis (Schuppan and Afdhal, 2008). Liver fibrosis is a reversible wound-healing process that is aimed at maintaining organ integrity, and presents as the critical pre-stage of liver cirrhosis. Liver cirrhosis, however, is an irreversible damage status accompanied by severe distortion of the liver vascular architecture.

Morbidity and mortality of cirrhosis in developed countries are increasing, and it has been the 14th most common cause of death worldwide and it leads to 1.03 million deaths per year worldwide (Lozano et al., 2012). Depending upon the occurrence of clinical decompensating events, the 1-year mortality in cirrhosis varies from 1 % to 57 % (D'Amico et al., 2006). Furthermore, patients with compensated cirrhosis run a yearly risk of 2-7 % for decompensation and a 1-7 % risk to develop primary hepatocellular carcinoma (HCC) (Schuppan, 2015). Infection with hepatitis C virus, alcohol abuse, and, progressively, non-alcoholic fatty liver disease are the principal causes in developed countries; however, the most common cause in sub-Saharan Africa and most parts of Asia is infection with hepatitis B virus (Tsochatzis et al., 2014). The prevalence of cirrhosis is difficult to assess and probably higher than reported, because the initial stages are asymptomatic and the dysfunction is undiagnosed.

After acute injury, the complete mass and original architecture of liver can be restored in a relatively short interval even when a large fraction of the organ is destroyed by itself. In contrast, chronic liver injury, as triggered by different etiologies mentioned above, induces repetitive tissue damage, leading to impaired regenerative ability marked by an altered inflammatory infiltrate and a chronic wound healing response (Bataller and Brenner, 2005; Lee et al., 2015). In addition, apoptosis and/or necrosis of parenchymal cells and their replacement by extracellular matrix (ECM) are also included in the response to chronic injury. The wound healing process becomes pathogenic if it progressively replaces parenchyma with scar tissue and distorts the liver vascular architecture, although initially beneficial, leading to organ dysfunction eventually (Trautwein et al., 2015).

Although other processes and cells can make significant contributions to the progress of fibrosis, the hepatic stellate cell (HSC) is considered as the major fibrogenic cell following its trans-differentiation into an activated type in a process which is termed activation (Lee and Friedman, 2011). Storing vitamin A and probably to maintain the normal basement

membrane type matrix are the main functions of quiescent HSCs in normal liver, whereas, in response to liver injury, HSCs undergo the activation process accompanied by losing vitamin A, becoming highly proliferative, and synthesizing fibrotic ECM which is rich in collagen type I (COL1) (Reeves and Friedman, 2002).

Over the past 2 decades, numerous things have been clarified about the biology and pathophysiology of fibrosis. Understanding the mechanisms underlying fibrosis has indicated several possible therapeutic approaches. Preclinical researches have been especially informative, and have highlighted a lot of potential therapies which have primarily been etiology-driven by eliminating or ameliorating the causative agent of fibrosis or cirrhosis. Although therapies which are directed at the underlying disease process, including anti-viral therapies for patients with hepatitis B and hepatitis C virus infection, have proven to be effective at reducing and/or reversing fibrosis, effective and specific anti-fibrotic therapy remains elusive (Rockey, 2013).

Up to date, liver transplantation is the most efficacious therapy for acute liver failure and advanced cirrhosis, but its application is limited because of organ donor shortage, financial considerations, and the requirement for lifelong immunosuppression (Ward et al., 2018). An alternative approach such as stem cell transplantation has been suggested as an effective alternate therapy for hepatic disease (Zhang and Wang, 2013).

2. Hepatic stellate cells

HSCs are liver-specific pericytes within the vasculature of the hepatic sinusoid. Stellate cells were first described by the German anatomist Carl von Kupffer in 1876. In 1952, HSCs were defined by the Japanese anatomist Toshio Ito as fat-storing cells by confirming the existence of cytoplasm lipid droplets (Ito and Nemoto, 1952). With the explosive growth in studies of HSCs, various names, such as perisinusoidal cells, pericytes, interstitial cells, lipocytes, fat-storing cells, Ito cells, or vitamin A-storing cells have been given on it (Geerts, 2001; Ito and Nemoto, 1952). So as to get rid of the confusion caused by its various names, standardization of the nomenclature as “hepatic stellate cells” took place in 1996 (Ahern et al., 1996).

HSCs are the major nonparenchymal element and constitute around 10-15 % of the total number of resident cells in normal liver including hepatocytes (Geerts, 2001). HSCs are located in the perisinusoidal space of Disse between the epithelial hepatocytes and fenestrated liver endothelium. HSCs display a dendritic morphology and embrace the endothelial cell layer of the sinusoids with thorn-like micro-projections providing physical

contact not only to sinusoidal endothelial cells but also with the cell body to the hepatocytes (Hellerbrand, 2013).

The most typical feature of HSCs in normal liver is their role in storage and transport of vitamin A. HSCs store 80 % of total body retinol as retinyl esters in the lipid droplets in the cytoplasm and regulate both vitamin A storage and transport (Blomhoff and Blomhoff, 2006). Moreover, vitamin A autofluorescence excited by 328 nm ultraviolet is a crucial feature of HSCs and is used for identifying HSCs.

Likewise, HSCs contribute to the three-dimensional architecture of the normal liver. They regulate the ECM turnover in the space of Disse by secreting adequate amounts of ECM molecules accompanied by secreting degrading enzymes called metalloproteinases (MMPs) and their inhibitors-tissue inhibitor of metalloproteinases (TIMPs) (Tacke and Weiskirchen, 2012).

Furthermore, HSCs play other pretty important roles in maintaining function of liver. For instance, HSCs are involved in the regulation of sinusoidal tone and are regarded as the principal cells that are implicated in sinusoidal blood flow regulation at present (Reynaert et al., 2008), and HSCs display immunological properties such as hepatic tolerance modulation (Su et al., 2012).In addition, HSCs are critical regulators of liver regeneration as it occurs after partial hepatectomy (Chen et al., 2012).

Under physiological conditions in the normal liver, HSCs reside in a quiescent stage and perform the proper functions that are mentioned above. However, following liver injury, HSCs undergo an activation process to a highly proliferative, myofibroblast-like cell type. HSC activation in diseased liver is characterized morphologically by loss of vitamin A droplets, ruffled nuclear membrane, enlargement of rough-surfaced endoplasmic reticulum and appearance of contractile filaments (Friedman, 2008). The expression of the cytoskeletal protein alpha-smooth muscle actin (α-SMA) is increased, which confers multiplied contractile potential, and α-SMA is admitted as a marker of activated HSCs (Bataller and Brenner, 2005; Tacke and Weiskirchen, 2012).

Activated HSCs synthesize and secrete a great quantity of ECM components such as collagen, glycosaminoglycan, proteoglycan, and glycoprotein (Gressner et al., 1994). Deposition of ECM is further enhanced by the production of TIMPs, which inhibit the degradation of ECM, resulting in a net accumulation of ECM with gradually disrupting normal liver architecture (Mormone et al., 2011).

During the activation of HSCs, there also occurs dramatically varied and enhanced expression and secretion of lots of pro- and anti-inflammatory cytokines and growth factors (Bataller and Brenner, 2005; Tacke and Weiskirchen, 2012). The most potent inducer of the

expression of collagen I and other ECM constituents by HSCs is transforming growth factor-β (TGFβ). Besides, platelet-derived growth factor (PDGF) is a potent inducer of HSC proliferation. Both factors, as well as their corresponding receptors, are *de novo* expressed during HSC activation (Bataller and Brenner, 2005; Friedman, 2008; Tacke and Weiskirchen, 2012). Generally, autocrine signaling is a critical process during HSC activation, underscoring the importance of tightly regulated local control of growth factor action and cytokine within the pericellular milieu (Friedman, 2008).

The activation of HSCs is the key event of hepatic fibrogenesis. Fibrosis during chronic disease can be regarded as deregulated wound healing. Persistent hepatocellular injury leads to acceleration and perpetuation of HSC activation with impaired ECM degradation and increased ECM synthesis. Increased net ECM deposition gives rise to a gradual disruption of normal liver architecture and ultimately liver cirrhosis (Bataller and Brenner, 2005; Mormone et al., 2011).

COL1 is the best studied ECM component of liver fibrosis, the expression of which is regulated both transcriptionally and post-transcriptionally in HSCs. Together with other HSC-produced ECM constituents such as adhesive glycoproteins and sulfated proteoglycans, COL1 forms the fibrotic bands that surround nodules in cirrhotic livers (Mormone et al., 2011; Tacke and Weiskirchen, 2012).

Activated HSCs are also significant mediators of hepatic immunoregulation. They initiate and amplify hepatic inflammation by the secretion of numerous different chemokines and cytokines, which advance differentiation of liver macrophages with pro-inflammatory as well as pro-fibrotic functions (Bataller and Brenner, 2005; Chang et al., 2013; Marra, 2002). Moreover, activated HSCs modulate the hepatic immune response by their expression of the costimulatory molecules (Muhlbauer et al., 2006).

Apart from their critical role in hepatic fibrosis and inflammation, activated HSCs play a role in the pathogenesis of portal hypertension. Activated HSCs respond by contraction to vasoactive substances according to their myofibroblastic phenotype (Reynaert et al., 2008). The acquisition of a contractile phenotype during HSC activation has been documented both *in vitro* and *in vivo*. Both the anatomical location of HSCs and the capacity to contract or unwind in response to numerous vasoactive mediators indicate that activated HSCs are major determinant of increases in portal resistance during liver fibrosis, no matter early or late (Hellerbrand, 2013).

3. Mesenchymal stem cells

Mesenchymal stem cells (MSCs) are stromal cells exhibiting the ability of multilineage differentiation and carry the capacity to self-renew. Bone marrow-derived MSCs (BM-MSCs), first discovered by Friedenstein in 1976 and described as undifferentiated MSCs in 1987, are still the most frequently investigated cell type and often designated as the gold standard (Friedenstein, 1976; Friedenstein et al., 1987). In recent years, evidence suggests that adult MSCs are present in nearly all human tissues, including adipose tissue (Fraser et al., 2006), peripheral blood (Cao et al., 2005) or lung (Griffiths et al., 2005); besides, MSCs have also shown promising potential for proliferation and differentiation into different cell types. In addition to distinct adult tissues such as bone marrow, adipose tissue and peripheral blood, MSCs can be obtained from several birth-associated tissues including placenta, amnion, umbilical cord and cord blood as well (Hass et al., 2011). A significant advantage of these neonatal tissues is their ready availability, therefore, avoiding invasive procedures and ethical problems. Furthermore, birth-associated tissues harbor a variety of embryonic or premature cell populations including MSCs, hematopoietic stem cells and endothelial stem/progenitor cells, which also suggested that MSCs from these neonatal tissues may have additional capacities in comparison to MSCs derived from adult sources. Indeed, several studies have reported superior cell biological properties such as enhanced proliferative capacity, life span and differentiation potential of MSCs from birth-associated tissues over BM-MSCs (Barlow et al., 2008; Brooke et al., 2008; In 't Anker et al., 2004).
Human MSCs are plastic-adherent cells differentiating into cells which originate from the endoderm and ectoderm (Liras, 2010; Lv et al., 2014; Wei et al., 2013). Moreover, they can abandon their undifferentiated or unspecialized states and transform into other mesenchymal lineages. Thus, they can regenerate cartilage, bone and fat and even turn into muscle cells, endothelial cells or neurons under physiological and experimental conditions (Lv et al., 2014; Wei et al., 2013).

As MSCs take responsibility for tissue repair, growth, wound healing and cell substitution resulting from physiological or pathological causes, they have various therapeutic application, for example, in the treatment of central nervous system afflictions like spinal cord lesions (Wei et al., 2013). Furthermore, by reason of their differentiation capacity, MSCs have become the *de facto* model for regenerative medicine study (Liras, 2010; Lv et al., 2014; Stanko et al., 2014). In the field of regenerative medicine, MSCs own several advantages over other types of stem cells. For instance, from an ethical viewpoint, the controversy surrounding the procurement of embryonic stem cells is virtually nonexistent in the case of MSCs or induced pluripotent stem cells, although teratogenicity limits the widespread use of the latter cell type (Lv et al., 2014; Stanko et al., 2014; Wei et al., 2013).

Recently, the concept of MSCs has been expanded to include the secretion of biologically active molecules which exert beneficial effects on other cells (Caplan and Dennis, 2006). This shifts a paradigm that is centered on differentiation to a view in which MSCs can be therapeutic even if they do not engraft or differentiate into tissue-specific cells, which increases the range of therapeutic applications of MSCs significantly. Paracrine effects of MSCs can be divided into trophic, immunomodulatory, anti-scarring and chemoattractant. The trophic effects of MSCs can be further subdivided into anti-apoptotic, supportive (stimulation of mitosis, proliferation and differentiation of stem cells or organ-intrinsic precursor) and angiogenic. The capacity to preferentially locate at sites of injured tissues, which may be affected by several factors (Karp and Leng Teo, 2009), adds to the regenerative properties of MSCs as it increases the possibility of systemically delivered cells finding the areas where their paracrine effects are most required, and this is of particular interest for clinical applications (Meirelles Lda et al., 2009).

In patients with cirrhosis or liver failure, fibrosis and inflammation-associated liver damage are usually mediated by abnormal innate and adaptive immune responses. Although many details of the involvement of MSCs with fibrotic and inflammatory processes stay unknown, MSCs have been demonstrated to play an immunomodulatory role through producing inhibitory cytokines or inducing the development of regulatory T cells (Sun et al., 2009). MSC therapy interestingly appears to be effective in regulating the immune response in tissue injury, transplantation, and autoimmunity in both animal models of liver disease and patients in clinical trials (Uccelli et al., 2008). MSCs can also directly inhibit the activation of HSCs via MSC-derived tumor necrosis factor alpha (TNF-α) and interleukin 10 (IL-10), and may also induce HSC apoptosis via, in part, the Fas/FasL pathway (Akiyama et al., 2012). Notably, MSCs have the potential to differentiate into myofibroblasts, which act as scar-forming cells within the liver in certain settings. Moreover, MSCs can differentiate into hepatocyte-like cells both *in vitro* and *in vivo* (Kia et al., 2013; Shu et al., 2004; Si-Tayeb et al., 2010) and can secrete trophic factors, including growth factors, cytokines and chemokines, which promote the regeneration of the impaired liver. Thus, MSCs are considered to act through multiple mechanisms to coordinate a dynamic, integrated response to liver inflammation and fibrosis, which prevents the progressive distortion of hepatic architecture, and to be a potential source for the treatment of liver fibrosis and cirrhosis (Zhang and Wang, 2013).

4. Purpose of this study

Recently, some types of MSCs have been used for developing treatments for fibrosis and human amnion-derived MSC (hAMSC) transplantation ameliorated liver fibrosis in rats in a previous study (Kubo et al., 2015); however, MSCs from different sources are not completely functionally identical and the mechanism of fibrosis amelioration induced by hAMSC is poorly understood. According to the feature of MSCs, the prevention of liver fibrosis is possibly achieved through secretory factors from MSCs. Thus, in this study, I investigated the effect of a conditioned medium obtained from hAMSC cultures (hAMSC-CM) on primary HSCs, and I also investigated the underlying mechanisms of its antifibrotic effect *in vitro*.

MATERIALS AND METHODS

1 Materials

The source of and methods for preparing the experimental materials used in this study are as follows.

1.1 Animals and Cells

Male SD rat (Japan SLC, Hamamatsu, Japan)

Human skin fibroblast C-12302 (PromoCell, Heidelberg, Germany)

1.2 Equipment

BD FACS Aria III Cell Sorter (BD Biosciences, San Jose, CA, USA)

BD FACS Canto II Flow Cytometer (BD Biosciences, San Jose, CA, USA)

Luna automated cell counter (Logos Biosystems, Anyang, South Korea)

Inverted fluorescence & phase contrast tissue culture microscope IX70 (Olympus, Tokyo, Japan)

FluoView FV10i confocal laser scanning microscope (Olympus, Tokyo, Japan)

Veriti 96-well Thermal Cycler (Applied Biosystems, Waltham, MA, USA)

Step One Plus Real Time PCR System (Applied Biosystems, Waltham, MA, USA)

NanoDrop 2000 Spectrophotometers (Thermo Fisher Scientific, Waltham, MA, USA)

GloMax-Multi+ Detection System (Promega, Fitchburg, WI, USA)

SpectraMax Paradigm Multi-Mode Detection System (Molecular Devices, San Jose, CA, USA)

Soft Incubator SLI-450ND (Eyela, Tokyo, Japan)

Soft Incubator SLI-600ND (Eyela, Tokyo, Japan)

Direct heat CO_2/multi-gas incubator SCA-165D (Astec, Fukuoka, Japan)

Tabletop micro refrigerated centrifuge 3520 (Kubota, Tokyo, Japan)

High speed refrigerated centrifuge SRX-201 (Tomy, Tokyo, Japan)

High capacity refrigerated centrifuge 8910 (Kubota, Tokyo, Japan)

Perista Pump SJ-1211 (Atto, Tokyo, Japan)

Universal Shaker SHK-U4 (Iwaki, Tokyo, Japan)

Constant temperature bath SB-9 (EYELA, Tokyo, Japan)

1.3 Kits

Human MSC Analysis Kit (BD Biosciences, San Jose, CA, USA)

RNeasy Mini Kit (Qiagen, Hilden, Germany)
PrimeScript RT Reagent Kit with a gDNA Eraser (Takara Bio, Kusatsu, Japan)
CCK-8 (Dojindo Laboratories, Kumamoto, Japan)
COL1 ELISA kit (MyBioSource, San Diego, CA, USA)
TGFβ1 ELISA kit (R&D Systems, Minneapolis, MN, USA)
Rat surgical kit

1.4 Culture Media and Culture-associated Materials

MEMα (Nacalai Tesque, Kyoto, Japan)
Phenol red–free MEMα (Nacalai Tesque, Kyoto, Japan)
DMEM (Nacalai Tesque, Kyoto, Japan)
SteCM (ScienCell, Carlsbad, CA, USA)
SteCGS (ScienCell, Carlsbad, CA, USA)
FBS (Thermo Fisher Scientific, Waltham, MA, USA)
Recombinant mouse TGFβ1 protein (R&D Systems, Minneapolis, MN, USA)
Penicillin (Wako Pure Chemical Industries, Osaka, Japan)
Streptomycin (Wako Pure Chemical Industries, Osaka, Japan)
PBS (Thermo Fisher Scientific, Waltham, MA, USA)
HBSS (–) (Nacalai Tesque, Kyoto, Japan)
HBSS (+) (Nacalai Tesque, Kyoto, Japan)
Costar 12-well cell culture plate (Corning, Corning, NY, USA)
Costar 96-well cell culture plate (Corning, Corning, NY, USA)
Nunc 35 mm cell culture dish (Thermo Fisher Scientific, Waltham, MA, USA)

1.5 Antibodies and Stain-related Reagents

Rabbit anti-rat α-SMA (Abcam, Cambridge, UK)
Rabbit anti-rat DESNIN (Abcam, Cambridge, UK)
FITC-conjugated mouse anti-rat CD31 (Bio-Rad, Hercules, CA, USA)
FITC-conjugated mouse anti-human CD163 (MBL, Nagoya, Japan)
Alexa Flour 488–conjugated anti-rabbit (Cell Signaling Technology, Danvers, MA, USA)
Rabbit IgG isotype control (GeneTex, Irvine, CA, USA)
FITC-conjugated mouse IgG isotype control (MBL, Nagoya, Japan)
Hoechst 33342 (Thermo Fisher Scientific, Waltham, MA, USA)
7-AAD (BD Biosciences, San Jose, CA, USA)

1.6 qRT-PCR-related Materials

Primer (Hokkaido System Science, Sapporo, Japan)

Platinum SYBR Green PCR Mix (Invitrogen, Thermo Fisher Scientific, Waltham, MA, USA)

8-well PCR tube strips with caps (BMBio, Tokyo, Japan)

96 well plate (0.1 mL) (Applied Biosystems, Waltham, MA, USA)

1.7 Software

ImageJ software (imagej.nih.gov/ij/)

Graph Pad Prism 7.0 (GraphPad Software, La Jolla, CA, USA)

1.8 Others

18 G needle (Terumo, Tokyo, Japan)

Dropper (Terumo, Tokyo, Japan)

FALCON cell strainer (Corning, Corning, NY, USA)

225 cm^2 tissue culture flask (Iwaki, Tokyo, Japan)

Pentobarbital sodium (Kyoritsu Seiyaku, Tokyo, Japan)

EDTA (Thermo Fisher Scientific, Waltham, MA, USA)

0.25% Trypsin/EDTA (Wako Pure Chemical Industries, Osaka, Japan)

0.5% Trypsin/EDTA (Wako Pure Chemical Industries, Osaka, Japan)

Collagenase II (Worthington Biochemical, Lakewood, NJ, USA)

DNase I (Worthington Biochemical, Lakewood, NJ, USA)

Brightase (Nippi, Tokyo, Japan)

Dispase (Wako Pure Chemical Industries, Osaka, Japan)

Percoll (GE Healthcare Bio-Science, Uppsala, Sweden)

Distilled water (Thermo Fisher Scientific, Waltham, MA, USA)

MeOH (Wako Pure Chemical Industries, Osaka, Japan)

EtOH (Wako Pure Chemical Industries, Osaka, Japan)

Preparation of 70 % (v/v) EtOH (50 mL):

EtOH	35 mL
Distilled water	Add in EtOH to a total volume of 50 mL

NaCl (Wako Pure Chemical Industries, Osaka, Japan)

Preparation of 1.5 M NaCl solution (50 mL):

NaCl	4.38 g
Distilled water	Dissolve NaCl to a total volume of 50 mL

HCl (Wako Pure Chemical Industries, Osaka, Japan)

Preparation of 1 N HCl (100 mL):

HCl	Add 8.33 mL of 12 N HCL in distilled water slowly.
Distilled water	91.67 mL

NaOH (Sigma-Aldrich, St.Louis, MO, USA)

HEPES (Thermo Fisher Scientific, Waltham, MA, USA)

Preparation of 1.2 N NaOH/0.5 M HEPES (100 mL):

NaOH	Add 12 mL of 10 N NaOH in 75 mL distilled water slowly.
HEPES	11.9 g
Distilled water	Bring final volume to 100 mL.

2 Methods

The Medical Ethical Committee of Hokkaido University, Graduate School of Medicine, Sapporo, Japan approved this study. The Animal Care and Use Committees of Hokkaido University approved the experimental protocol and animal care.

2.1 Animal Breeding

Male Sprague–Dawley (SD) rats (400–450 g in weight) were housed in a temperature-controlled room (24 °C) on a 12-hourly light–dark cycle and were provided with standard chow and water *ad libitum* until the time of the study.

2.2 Isolation and Expansion of Human Amnion-derived Mesenchymal Stem Cells (hAMSCs)

A pregnant woman provided written informed consent for use of her fetal membrane, which was obtained during her cesarean delivery. Isolation and expansion of hAMSCs were performed as follows. Amnion tissue was manually peeled from the chorion and hAMSCs were isolated and expanded by digestion using brightase and dispase. hAMSCs were then seeded into plastic dishes containing Minimum essential medium alpha (MEMα) supplemented with 10 % (v/v) fetal bovine serum (FBS), 100 U/mL penicillin, and 100 μg/mL streptomycin. Cell cultures were maintained at 37 °C in a humidified atmosphere of 95 % (v/v) air and 5 % (v/v) carbon dioxide (CO_2). After 3–4-days culture, non-adherent cells were removed and adherent cells were cultured to 80 % confluence. Passage was performed using 0.5 % trypsin/ethylenediaminetetraacetic acid (EDTA). The expanded hAMSCs were stored in liquid nitrogen until use.

2.3 Preparation of Conditioned Medium Obtained from Human Amnion-derived Mesenchymal Stem Cell Cultures (hAMSC-CM)

Cryopreserved hAMSCs (passage 5) were recovered and cultured in MEMα containing 10 % (v/v) FBS, until the cells reached a sub-confluent state. After washing them with Hank's balanced salt solution without calcium, magnesium, or phenol red (HBSS (–)), the cells were further cultured with serum-free MEMα for 48 hours. Next, the culture medium was collected with debris removing by centrifugation at 1120 × g for 5 minutes, using as hAMSC-CM. Serum-free MEMα incubated in a cell-free dish for 48 hours was used as a standard medium (SM), and both SM and hAMSC-CM were stored at −80 °C until use.

2.4 Preparation of Conditioned Medium Obtained from Skin Fibroblast Cultures (fibroblast-CM)

Cryopreserved human skin fibroblasts were recovered and cultured in MEMα containing 10 % (v/v) FBS, until the cells reached a sub-confluent state. After washing them with HBSS (–), the cells were further cultured with serum-free MEMα for 48 hours. Subsequently, the culture medium was collected with debris removing by centrifugation at 1120 × g for 5 minutes, using as fibroblast-CM, and was stored at −80 °C until use.

2.5 Isolation and Purification of Hepatic Stellate Cells (HSCs)

Previous studies have shown various methods of isolating HSCs (Bartneck et al., 2015; Liu et al., 2011; Mederacke et al., 2015; Zhang et al., 2016b); I performed isolation after modifying several steps. The SD rats were anesthetized by intraperitoneal injection of 6.48 mg/100 g body weight of pentobarbital sodium. Each rat's liver was perfused via the portal vein using an 18 G needle that was fixed by sutures. Buffers were preheated to 42 °C and pumped into the liver using a peristaltic pump.

2.5.1 Liver Perfusion and Enzymatic Digestion

Initially, the liver was perfused with 60 mL of HBSS (–) containing 1 mM EDTA at 18 mL/min, and when the liver became distended, the inferior vena cava (IVC) was cut. After that, the diaphragm was incised and the intrathoracic IVC was clipped with a vascular clamp to ensure the buffers were drained completely via the abdominal IVC incision. Next, the liver was infused with 200 mL of HBSS (–) supplemented with 100 U/mL of collagenase II at 7.5 mL/min. The perfused liver was removed, minced using two tweezers in a sterile dish containing HBSS (–), and further digested in a flask containing 65 U/mL of collagenase II and 1 % (v/v) of Deoxyribonuclease I (DNase I) with the stock solution concentration of 40

KU/mL which was prepared by Hank's balanced salt solution with calcium, magnesium, but without phenol red (HBSS (+)) immediately before use. The flask was placed on a stir plate and shaken at 70 rpm for 20 minutes in an incubator at 37 °C. The resulting cell suspension was filtered using first a 100 μm and then a 70 μm cell strainer and was centrifuged for 10 minutes at 600 × g and 4 °C. The pellet was washed and resuspended using 50 mL HBSS (–) containing 120 μL of DNase I solution and then centrifuged for 3 minutes at 50 × g and 4 °C. Then, the supernatant was collected and centrifuged for 10 minutes at 400 × g and 4 °C.

2.5.2 Density Gradient Centrifugation

The pellet was resuspended in 7 mL HBSS (−) containing 24 μL of DNase I solution and, then, was mixed with Percoll solution (prepared by Percoll and 1.5 M Sodium chloride (NaCl) solution at the ratio of 9:1) to a final concentration of 30 % (v/v) at 20°C. Next, 10 mL of a thoroughly mixed cell–Percoll suspension was pipetted into a 15 mL centrifugation tube, and 2 mL of HBSS (–) was gently overlaid on the suspension. Centrifugation was performed at 1470 × g and 20 °C for 25 minutes with slow acceleration and deceleration. The interphase containing enriched HSCs between HBSS (−) and the 30 % Percoll layer was harvested and washed using HBSS (−) for 8 minutes at 400 × g and 4 °C.

2.5.3 Fluorescence-activated Cell Sorting (FACS) for HSCs

The HSC pellet was resuspended in phenol red–free MEMα supplemented with 1.5 % (v/v) FBS, and the suspension was filtered using a 40 μm cell strainer and adjusted to 6–8 × 10^6 cells/mL. A BD FACS Aria III Cell Sorter was used to perform HSC sorting. Endogenous retinoid fluorescence of HSCs was used as a selection marker, performed excitation via 375 nm LASER, and measured the emission using a 450/20 nm band-pass filter at Hoechst-blue channel. A 100 μm nozzle and a 2.0 neutral density filter were used, and the sample loading port was set to 4 °C, 300 rpm. The sorting mode was set up in purity mode, and 2 μL/10^6 cells of 7-aminoactinomycin D solution (7-AAD) was added to the suspension immediately before sorting. The 15 mL collection tube was made of polypropylene and was coated with FBS overnight at 4 °C. 10 mL of Dulbecco minimal essential medium (DMEM) supplemented with 17 % (v/v) FBS was contained in the tube to collect sorted cells, and after sorting, the cells were collected by centrifuging for 5 minutes at 400 × g and 4 °C for purity determination and cell culture.

2.6 HSC Culture Models

All the cells were cultured in a humidified atmosphere of 95 % (v/v) air and 5 % (v/v) CO_2 at 37 °C. All the culture media were supplemented with 100 U/mL of penicillin and 100 μg/mL of streptomycin. A Luna automated cell counter was used to take a cell count.

2.6.1 Routine Culture of HSCs

Approximately 5×10^4 HSCs were seeded on each well of 12-well plastic plates, on which the cells were automatically activated and proliferated (Osawa et al., 2013). They were cultured in 2 mL of stellate cell medium (SteCM) supplemented with 2 % (v/v) FBS and stellate cell growth supplement (SteCGS) for 48 hours. Then, the HSCs were washed thrice using HBSS (–) and were cultured for 48 hours with SM, fibroblast-CM or hAMSC-CM. In addition, hAMSC-CM was mixed separately with the SM in two concentrations: 50 % and 25 % (v/v) of hAMSC-CM. These different concentrations of hAMSC-CM were also used for culturing HSCs for 48 hours as described above

2.6.2 Transforming Growth Factor–beta (TGFβ) Treatment

Approximately 5×10^4 HSCs were cultured in 12-well plates in SteCM containing 2 % (v/v) FBS and SteCGS for 48 hours and washed thrice using HBSS (–). Subsequently, the HSCs were treated with SM or hAMSC-CM supplemented with 5 ng/mL of TGFβ1 for 48 hours. HSCs cultured in SM or hAMSC-CM for 48 hours served as negative controls.

2.7 Flow Cytometry Analysis

The cells were washed twice by HBSS (–) and harvested by 0.25 % trypsin/EDTA. After that, the suspension was centrifuged at 400 × g for 5 minutes and the pellet was resuspended by HBSS (–) and transferred into 1.5 mL centrifugation tube. Centrifugation was performed for 2 minutes at 400 × g and the supernatant was aspirated carefully. The pellet was fixed by pre-cooling Methanol (MeOH, -30 °C) for 5 minutes at 4 °C and then the cells were centrifugated and washed twice by phosphate buffered saline (PBS) at 400 × g for 2 minutes each time. PBS containing 1 % (w/v) bovine serum albumin (BSA) was used to block the cells for 30 minutes at room temperature. The cells were centrifugated and washed twice by PBS at 400 × g for 2 minutes each time and the following procedures were divided into two categories according to the different types of antibodies. (i) The cells were incubated with primary antibodies (or isotype controls) for 1 hour at room temperature. Next, the cells were washed twice by PBS at 400 × g for 2 minutes each time and then incubated with secondary antibodies for 30 minutes at room temperature in the dark, following twice wash by PBS at 400 × g for 2 minutes each time at last. (ii) The cells were incubated with fluorescein-

conjugated antibodies (or isotype controls) for 1 hour at room temperature in the dark and then were washed twice by PBS at 400 × g for 2 minutes each time. All the prepared cells were resuspended in HBSS (–), filtered using a 40 μm strainer, and then analyzed using a BD FACS Canto II Flow Cytometer.

2.7.1 Flow Cytometry Analysis of hAMSCs

Cultured hAMSCs were harvested with 0.5 % trypsin/EDTA and were stained using a Human Mesenchymal Stem Cell (MSC) Analysis Kit containing phycoerythrin (PE)-conjugated anti-cluster of differentiation (CD) 44, allophycocyanin (APC)-conjugated anti-CD73, fluorescein-isothiocyanate (FITC)-conjugated anti-CD90, and PerCP-Cy5.5-conjugated anti-CD105 antibodies, as well as a negative mixture comprising PE-conjugated anti-CD11b, anti-CD19, anti-CD34, anti-CD45, anti–Human leukocyte antigen–antigen DR (HLA-DR) antibodies and all the corresponding isotype control antibodies.

2.7.2 Flow Cytometry Analysis of HSCs

Sorted HSCs were harvest by centrifugation at 400 × g for 5 min and were stained using rabbit anti-rat DESMIN primary antibody (1:500), as well as Alexa Flour 488-conjugated anti-rabbit antibody (1:1,000). FITC-conjugated mouse anti-rat CD31 antibody (1:500), FITC-conjugated mouse anti-human CD163 antibody (1:500) were also used to stain the sorted HSCs in the manner as described above.

2.8 Immunofluorescent Staining

HSCs cultured in SM and hAMSC-CM were washed thrice using HBSS (–), fixed in pre-cooling MeOH (-30 °C) for 10 minutes at 4 °C. Then the cells were washed by HBSS (–) and incubated in anti-rat alpha–smooth muscle actin (α-SMA, 1:500) in HBSS (–) containing 2 % (v/v) FBS for 1 h at room temperature. After washing by HBSS (–) thrice, 5 minutes each time, the cells were incubated in Alexa Flour 488–conjugated anti rabbit secondary antibody (1:1,000) for 30 minutes at room temperature in the dark. Subsequently, the cells were washed by HBSS (–) and the nucleus was stained with Hoechst 33342 (1:1,000) for 3 minutes at room temperature. Then, the cells were washed twice and covered by PBS and analyzed using a FluoView FV10i confocal laser scanning microscope, all the micrographs were taken under the same exposure time and laser intensity. ImageJ software was used to measure fluorescence intensity.

2.9 Ribonucleic Acid (RNA) Isolation

RNA of the cultured cells was extracted using a RNeasy Mini Kit. After washing cells with HBSS (–), 350 μL Buffer RLT was added into the well, following pipetting several times. 350 μL 70% (v/v) Ethanol (EtHO) was added to the lysate, and was mixed well by pipetting. The 700 μL mixture was transferred to a RNeasy Mini spin column placed in a 2 mL collection tube, and was centrifugated for 1 minute at 8000 × g. The flow-through was discarded and 700 μL Buffer RW1 was added to the RNeasy Mini spin column, following centrifugation for 1 minute at 8000 × g. Then the flow-through was discarded and 500 μL Buffer PRE was added to the RNeasy Mini spin column. After centrifugation for 1 minute at 8000 × g, the flow-through was discarded. Next, 500 μL Buffer PRE was added to the RNeasy Mini spin column and was centrifugated for 2 minutes at 8000 × g. Subsequently, the RNeasy Mini spin column was placed in a new 2 mL collection tube and was centrifugated for 1 min at full speed to dry the membrane. At last, the RNeasy Mini spin column was placed in a new 1.5 mL collection tube and 50 μL RNase-free water was added directly to the spin column membrane, following centrifugation for 1 minute at 8000 × g to elute the RNA. The concentration of isolated RNA was measured with a NanoDrop 2000 Spectrophotometer.

2.10 Quantitative Reverse-transcription Polymerase Chain Reaction (qRT-PCR)

Genomic deoxyribonucleic acid (gDNA) was eliminated and RNA was reverse-transcribed into complementary deoxyribonucleic acid (cDNA) using a PrimeScript RT Reagent Kit with gDNA Eraser. (i) gDNA Eraser and 5X gDNA Eraser Buffer were mixed at a ratio of 1:2, and the RNA solution which could be adjusted concentration by distilled water was added in the mixture at a ratio of 7:3 to a final volume of 10 μL. The mixed solution should be stay at room temperature for at least 5 minutes, but no more than 30 minutes, to clean up the gDNA. (ii) Afterwards, 5X PrimeScript Buffer 2, RT Primer Mix, PrimeScript RT Enzyme Mix 1 and RNase Free dH_2O were mixed at a ratio of 4:4:1:1 to a total volume of 10 μL. (iii) 20 μL solution gotten by mixing (i) and (ii) was added in 8-well polymerase chain reaction (PCR) tube strips with caps, and then total RNA were transcribed into cDNA in a Veriti 96-well Thermal Cycler, incubated at 37 °C for 15 minutes and 85 °C for 15 sesconds. PCR was carried out in a total reaction volume of 25 μL containing 5 μL of template cDNA mixture, 12.5 μL of a Platinum SYBR Green PCR Mix, and 2 μL of a 10 μM corresponding primer mixture in a 96-well plate (0.1 mL). PCR conditions, running on a Step One Plus Real Time PCR System, included pre-denaturation at 95 °C for 20 seconds followed by 40 cycles at 95 °C for 3 seconds and 60 °C for 7 seconds. A melting curve was created to validate the specificity of the amplification products. A relative expression was determined using the relative standard curve method with Platelet-derived growth factor receptor beta (*Pdgfrb*)

(Mederacke et al., 2015) or 18S ribosomal ribonucleic acid (*18s rrna*) used as an endogenous control for rat cells and *18S rRNA* for human cells. Table 1 shows the primer sequences.

Table 1 Sequences of primers

Gene	Forward primers (5'–3')	Reverse primers (5'–3')
α-Sma	GACACCAGGGAGTGATGGTT	GTTAGCAAGGTCGGATGCTC
Col1a1	GATGGCTGCACGAGTCACAC	ATTGGGATGGAGGGAGTTTA
Mmp-2	CTTGCTGGTGGCCACATTC	CTCATTCCCTGCGAAGAACAC
Mmp-9	CGCTCATGTACCCCATGTATCA	TCAGGTTTAGAGCCACGACCAT
Mmp-13	TCGCATTGTGAGAGTCATGCCAACA	TGTGGTTCCAGCCACGCATAGTCA
Timp-1	GACCACCTTATACCAGCGTT	GTCACTCTCCAGTTTGCAAG
Timp-2	GGATGGACTGGGTCACAGAG	GCGCAAGAACCATCACTTCT
Ccnb-1	CCCTACCAAAACCTGTGGAC	CATCGGAGAAAGCCTGACAC
Ccnb-2	TGGAGAGTGAAATACTGGAAGTCA	TGAGAAGCACACGATGGAAG
Tgfbr1	ACCTTCTGATCCATCCGTT	CGCAAAGCTGTCAGCCTAG
Pdgfrb	GCACCGAAACAAACACACCTT	ATGTAACCACCGTCGCTCTC
Clec4f	ACGGAGAGCGTGAAGACTGT	CTTGCACACCCAGTTGTAGG
Albumin	TGTCCCCAAAGAGTTTAAAGCTG	TCTTTATCTGCTTCTCCTTGTCTGG
18s rrna	GCAATTATTCCCCATGAACG	GGCCTCACTAAACCATCCAA
IGTA11	TCACGGACACCTTCAACATGG	CCAGCCACTTATTGCCACTGA
CD26	AGTGGCGTGTTCAAGTGTGG	CAAGGTTGTCTTCTGGAGTTGG
18S rRNA	GATATGCTCATGTGGTGTTG	AATCTTCTTCAGTCGCTCCA

2.11 Proliferation Assay

Approximately 2×10^4 HSCs were cultured in a 96-well plate with SteCM containing 2 % (v/v) FBS and SteCGS for 48 hours. Then, the medium was changed to SM or hAMSC-CM and the cells were cultured for further 48 hours. HSC proliferation was examined using Cell Counting Kit-8 (CCK-8) at 0, 24, and 48 hours after changing the medium; the medium without cells was used as a blank control. A GloMax-Multi+ Detection System was used to measure absorbance (450 nm).

2.12 Collagen Type 1 (COL1) Assay

The COL1 concentration in cultured SM and hAMSC-CM was evaluated using a rat COL1 enzyme-linked immunosorbent assay (ELISA) kit according to the manufacturer's instructions in routine culture of HSCs. Cell-free SM and hAMSC-CM were incubated at the

same time and taken as blank controls to determine the baseline. The media were collected and then were centrifugated for 5 min at 1120 × g, following the supernatant was collected for testing. The ELISA kit was gotten out of refrigerator in advance and the test was taken when it balanced to room temperature. The washing buffer was made by diluting the concentrated washing solution (25X) with distilled water. Then COL1 standard sample was prepared as follows (i) 1 mL standard sample diluent was added into COL1 lyophilized standard sample and was kept still for 30 minutes. (ii) The standard sample was mixed slightly after it completely dissolved and then was taken dilution with standard sample diluent as needed (10, 5, 2.5, 1.25, 0.625, 0.312, 0.156 ng/mL), and standard sample diluent was used as a negative control. All the samples were diluted (3X) with sample diluent and 100 μL dilutions were added into corresponding wells of antibody precoated plate, as well as the prepared standard samples. The reaction wells were sealed with adhesive tapes and were hatched in incubator at 37 °C for 90 minutes after shaking for 1 minute. The ELISA plate was washed twice by adding 350 μL washing buffer to wells and keeping it still for 30 s each time. The concentrated biotinylated antibody was diluted (100X) with antibody diluent 30 minutes before use, and 100 μL dilutions were added to individual wells. The reaction wells were sealed with adhesive tapes and were hatched in incubator at 37°C for 60 minutes. The ELISA plate was washed thrice in the manner as described above. Afterwards, the concentrated enzyme-conjugate was diluted (100X) by enzyme-conjugate diluent 30 minutes in advance, and 100 μL dilutions were added to each well. The reaction wells were sealed with adhesive tapes and were hatched in incubator at 37 °C for 30 minutes, following washing the ELISA plate five times in the manner as described above. Colour reagent liquid was prepared with Colour Reagent A and Colour Reagent B by the proportion of 9:1, and 100 μL Colour reagent liquid was added to individual well, hatching in dark at 37 °C for 30 minutes. 100 μL Colour reagent C was added to individual well and was mixed well. A SpectraMax Paradigm multi-mode detection platform was used to measure absorbance (450 nm) within 10 minutes, and calculate the result.

2.13 TGFβ1 Assay

The TGFβ1 concentration in SM and hAMSC-CM was evaluated using a rat TGFβ1 ELISA kit according to the manufacturer's instructions before culturing HSCs. -80 °C stored SM and hAMSC-CM were used for testing. Before testing, the TGFβ1 sample had to be activated as follows (i) 1N HCL was added in the sample with a ratio of 1:5, then mixed them well and incubated for 10 minutes at room temperature. (ii) The acidified sample was neutralized by adding 1.2 N NaOH/0.5 M 4-(2-hydroxyethyl)-1-piperazineethanesulfonic acid (HEPES) with

a ratio of 6:1, then mixed them well and assay immediately. The ELISA kit was gotten out of refrigerator in advance and the test was taken when it balanced to room temperature. The control was prepared by adding 1 mL distilled water in TGFβ1 Control without activation procedure. The wash buffer was made by diluting the Wash Buffer Concentrate (25X) with distilled water. And Calibrator Diluent RD5-53 (1X) was prepared with distilled water by diluting the Calibrator Diluent RD5-53 (4X). Then TGFβ1 standard sample was prepared as follows (i) Calibrator Diluent RD5-53 (1X) was added into TGFβ1 Standard to a final concentration of 2,000 pg/mL, and the reconstituted solution was kept still for at least 5 min. (ii) The standard sample was mixed slightly after it completely dissolved and then was taken dilution with Calibrator Diluent RD5-53 (1X) as needed (2,000, 1,000, 500, 250, 125, 62.5, 31.3 pg/mL), and Calibrator Diluent RD5-53 (1X) was used as a zero standard (0 pg/mL). All the samples were diluted (5X) with Calibrator Diluent RD5-53 (1X) and 50 µL dilutions were added into corresponding wells of antibody precoated plate, as well as the prepared standard samples and control, and then 50 µL Assay Diluent RD1-21 was add to each well. The reaction wells were sealed with adhesive tapes and were incubated at room temperature for 2 hours after shaking for 1 minute. The ELISA plate was washed 4 times by adding 400 µL wash buffer to wells and keeping it still for 30 seconds each time. 100 µL of TGFβ1 Conjugate were added to individual wells and the reaction wells were sealed with new adhesive tapes and were incubated at room temperature for 2 hours. The ELISA plate was washed 4 times in the manner as described above. Afterwards, Substrate Solution was prepared with Color Reagent A and Color Reagent B by mixing them together in equal volumes within 15 minutes of use, and 100 µL Substrate Solution was added to individual well, protecting from light at room temperature for 30 minutes. 100 µL of Stop Solution was added to individual well and was mixed well. A SpectraMax Paradigm multi-mode detection platform was used to measure absorbance (450 nm) within 30 minutes, and calculate the result.

2.14 Statistical Analysis

Graph Pad Prism 7.0 was used to perform the statistical analysis, and the data were expressed as mean ± standard deviation (mean ± SD). Intergroup differences were identified using one-way analysis of variance (ANOVA), followed by the Tukey test. Unpaired t-tests or Welch's test was used to identify pairwise differences. The differences were considered statistically significant at $P < 0.05$.

3 Graphical Representation

The overall flow of this study is shown in Fig. 1 in a form of schematic diagram.

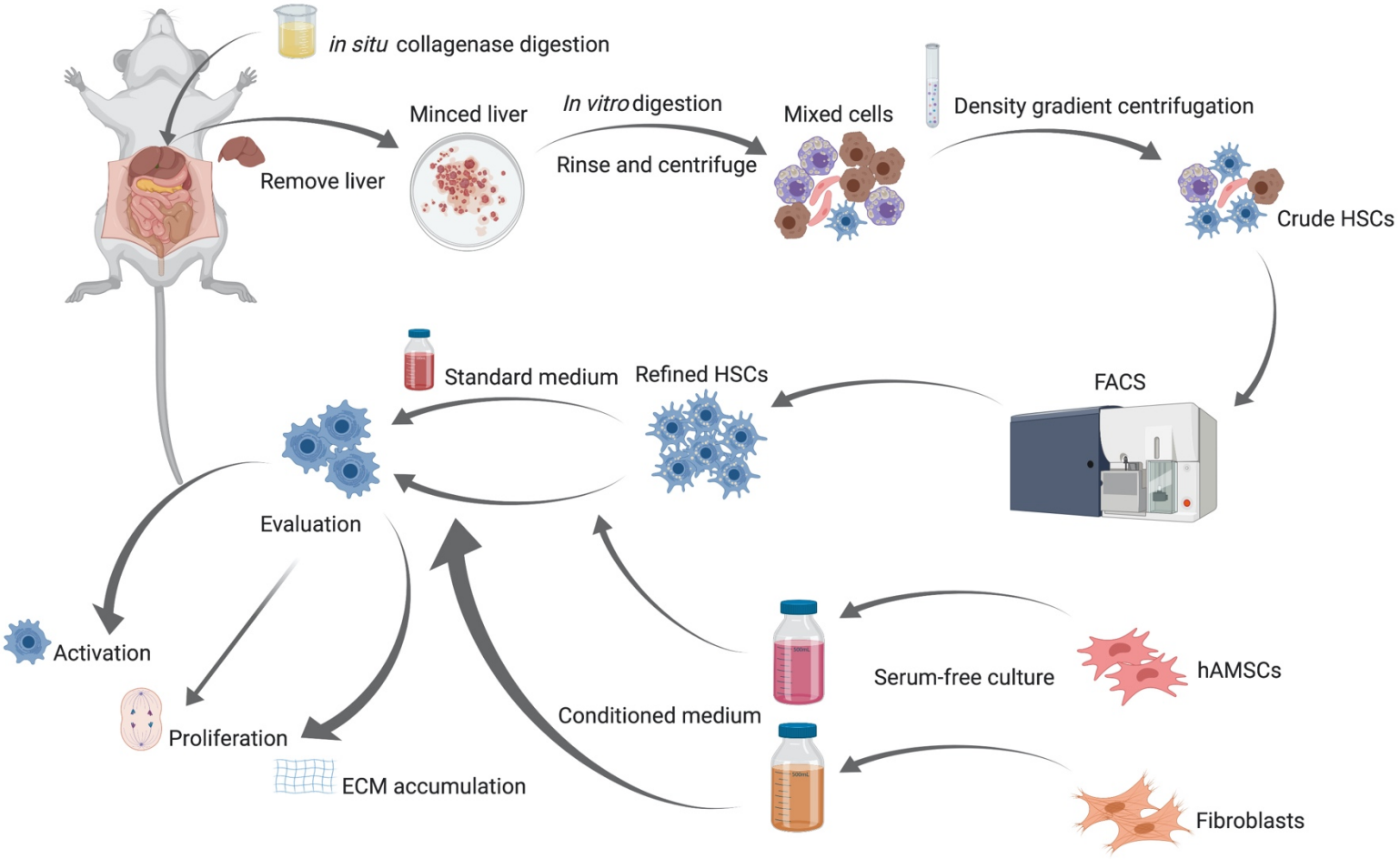

Figure 1. The overall flow chart of the study.

RESULTS

1 Characterization of hAMSCs

I observed that cultured hAMSCs have a typical morphology of fibroblast-like cells (Fig. 2). Flow cytometry showed that hAMSCs exhibit high expression of CD44, CD73, CD90, and CD105 but no expression of CD11b, CD19, CD34, CD45, or HLA-DR (Fig. 3), which is consistent with a characteristic of MSCs (Dominici et al., 2006; Parolini et al., 2008).By the way, a large numbers of fibroblast exist in the amnion as well, and it is difficult to distinguish between hAMSCs and fibroblasts by morphology alone or even widely accepted markers of hAMSCs. Some studies have proposed new approaches to differentiate these two types of cells (Kundrotas, 2012). In our study, hAMSCs and human skin fibroblasts were tested, and the high expression of MSC-specific marker integrin alpha 11 (*ITGA11*) and low expression of fibroblast-specific marker *CD26* in cultured hAMSCs indicated that fibroblast contamination is rarely observed in these hAMSCs (Fig. 4).

hAMSCs

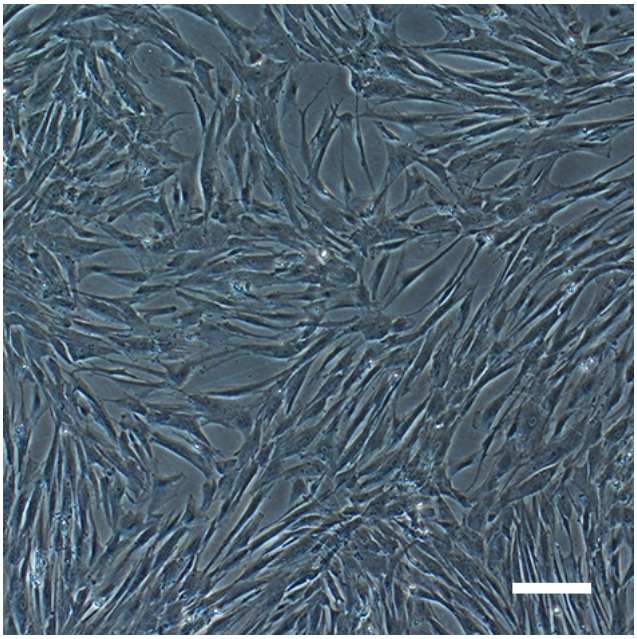

Figure 2. Characterization of cultured hAMSCs. Scale bars = 200 μm.

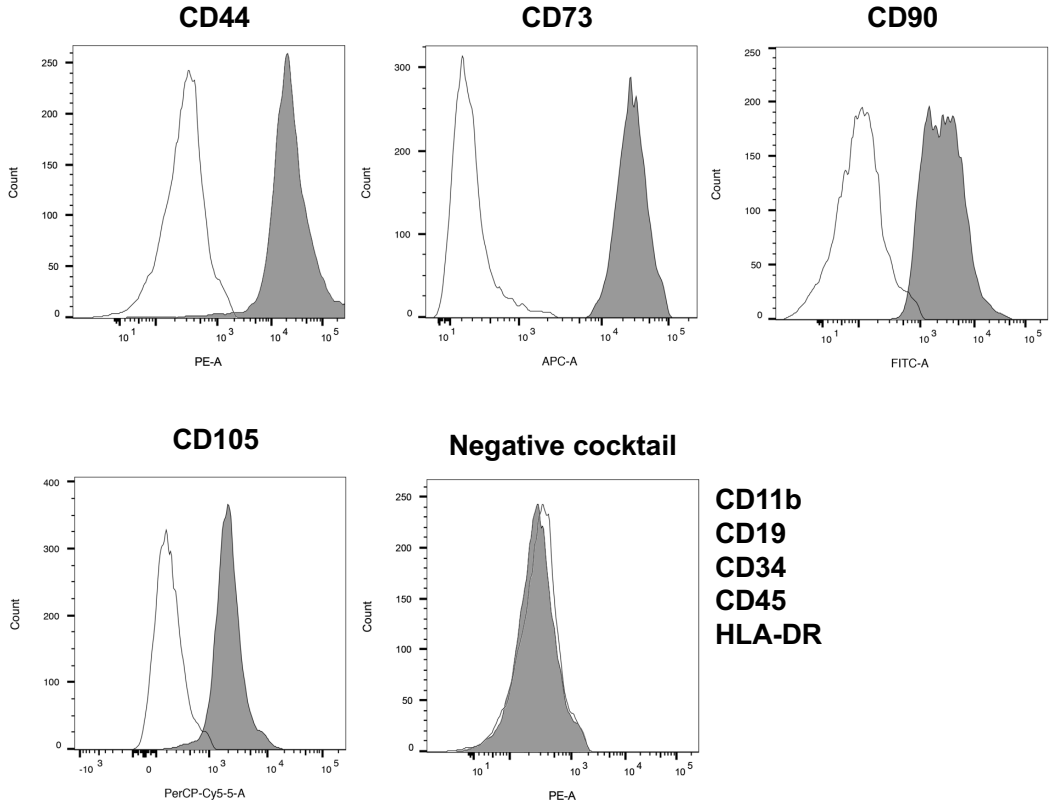

Figure 3. Flow cytometry analysis of cultured hAMSCs. Closed areas indicate staining with a specific antibody, whereas open areas represent staining with isotype control antibodies.

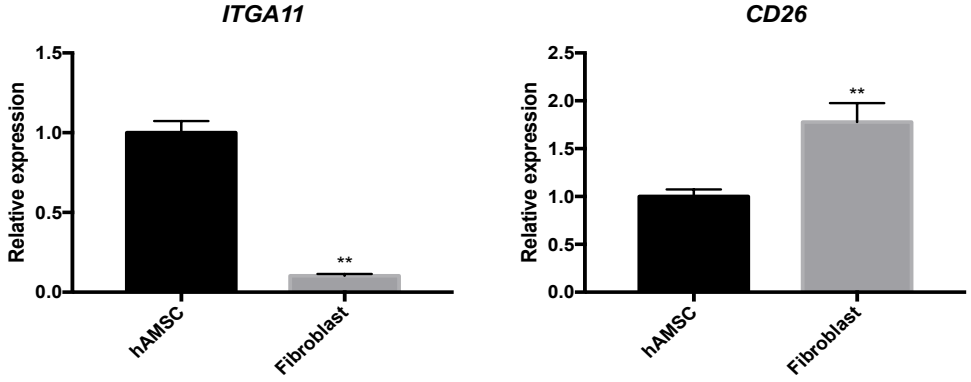

Figure 4. Expressions of MSC-specific gene *IGTA11* and fibroblast-specific gene *CD26* were examined in hAMSCs and skin fibroblasts by quantitative reverse-transcription polymerase chain reaction. Gene expression was normalized to *18S rRNA*. Data are shown as mean ± SD (n = 3). $^{**}P < 0.01$

2 Isolation and Characterization of HSCs

First, I gated cells with high sideward scatter (SSC) and forward scatter (FSC) (Geerts et al., 1998), and 7-AAD was used to select living cells (Fig. 5). I used the forward scatter area/forward scatter height (FSC-A/FSC-H) to exclude doublets, and a high autofluorescence area was gated as HSCs (Fig. 5). FACS of HSCs resulted in increasing the purity of HSCs, as defined by specific-gene and protein expression. High *Pdgfrb* expression and low C-type lectin domain family 4f (*Clec4f*), *Albumin* expression were showed in sorted cells, and remaining cells showed the opposite result (Fig. 6A). Moreover, the flow cytometry results showed that the sorted cells had high expression of DESMIN with the rate of 74.6 %, but no expression of CD31 and CD163 (Fig. 6B). A research indicated that not all the HSCs express DESMIN (Ballardini, 1994; March et al., 2007; Niki et al., 1996) even though DESMIN is wildly used for identifying HSCs. Thus, retinol-based autofluorescence was used to confirm the purity of sorted HSCs, exhibiting a final purity of > 98% (Fig. 7). The freshly isolated HSCs were irregularly round shaped, and their cytoplasm was rich in lipid droplets. When excited at 352 nm LASER, the vitamin A–rich lipid droplets emitted cyan intrinsic autofluorescence (Fig. 8). Post-culturing for 2 days, HSCs became extended and presented an asteroid phenotype, accompanied by a reduction of lipid droplets (Fig. 8). HSCs were further activated by routine culture, and it was difficult to observe autofluorescence post-culturing for 4 days (Fig. 8), suggesting that quiescent HSCs were activated by routine culture. Isolated HSCs proliferated well after seeding (Fig. 9A) and long-term culture showed that HSCs proliferated rapidly with good viability (Fig. 9B).

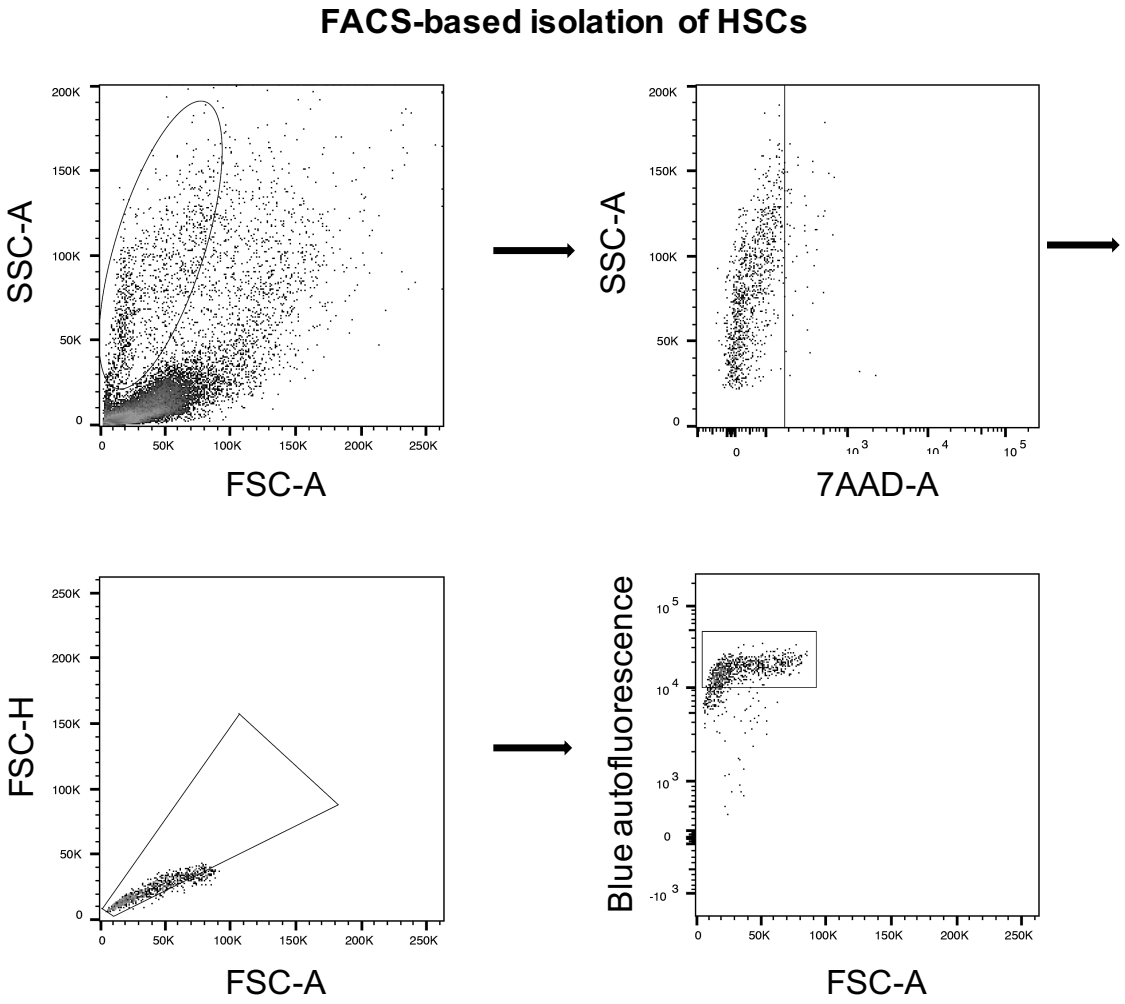

Figure 5. Gating strategy for HSC purification using FACS. Cells were gated on the basis of their FSC and SSC, viable cells were selected using 7-AAD, and doublets were excluded by FSC-A/FSC-H. Finally, HSCs were selected on the basis of the blue light emission from retinol.

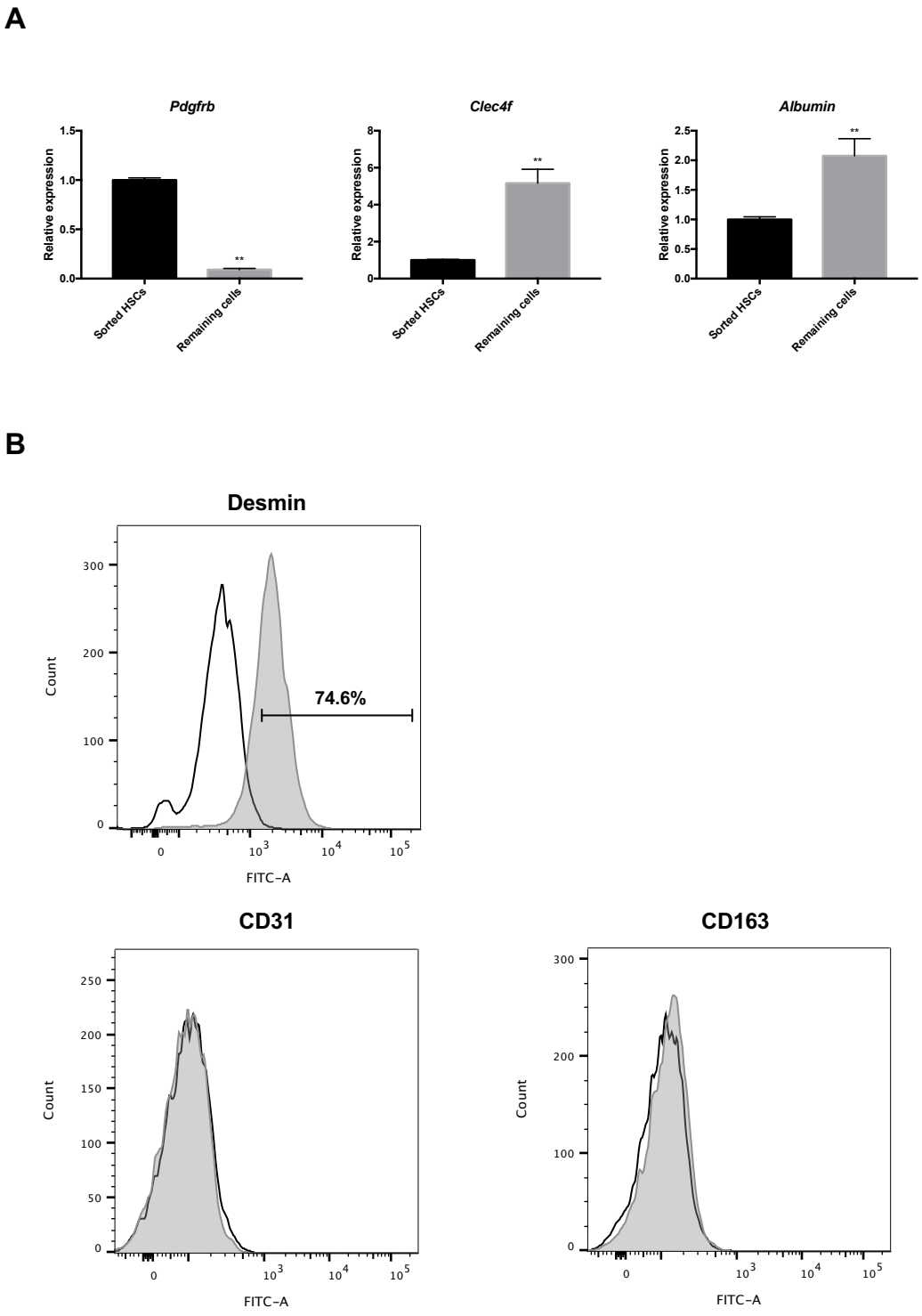

Figure 6. Characterization of sorted HSCs. (A) Cell type-specific gene expression analysis of sorted HSCs and remaining cells. *Pdgfb* is a marker of HSCs, *Clec4f* is a marker for Kupffer cells, and *Albumin* is a marker for hepatocytes. Data are expressed as mean ± SD ($n = 3$). $^{*}P < 0.05$; $^{**}P < 0.01$ versus sorted HSCs. (B) Desmin (HSC marker), CD31 (endothelial cell marker), CD163 (Kupffer cell marker) expression of sorted HSCs were analyzed by flow cytometry.

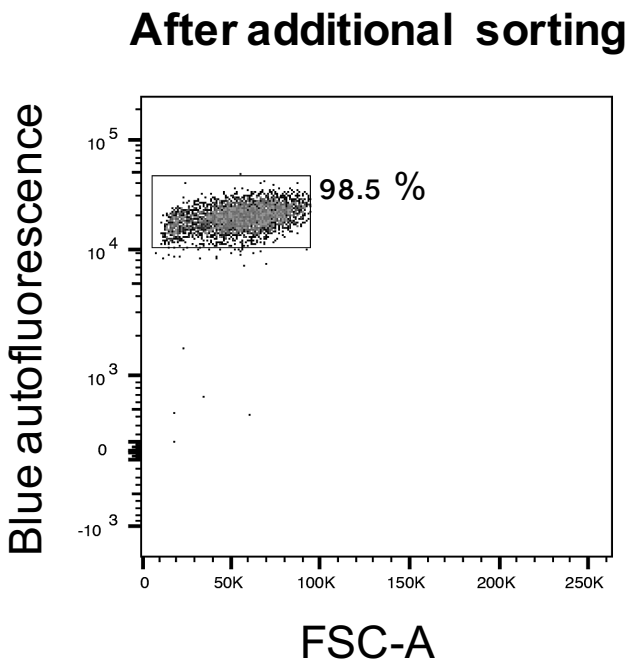

Figure 7. Purity of HSCs after FACS detected by autofluorescence.

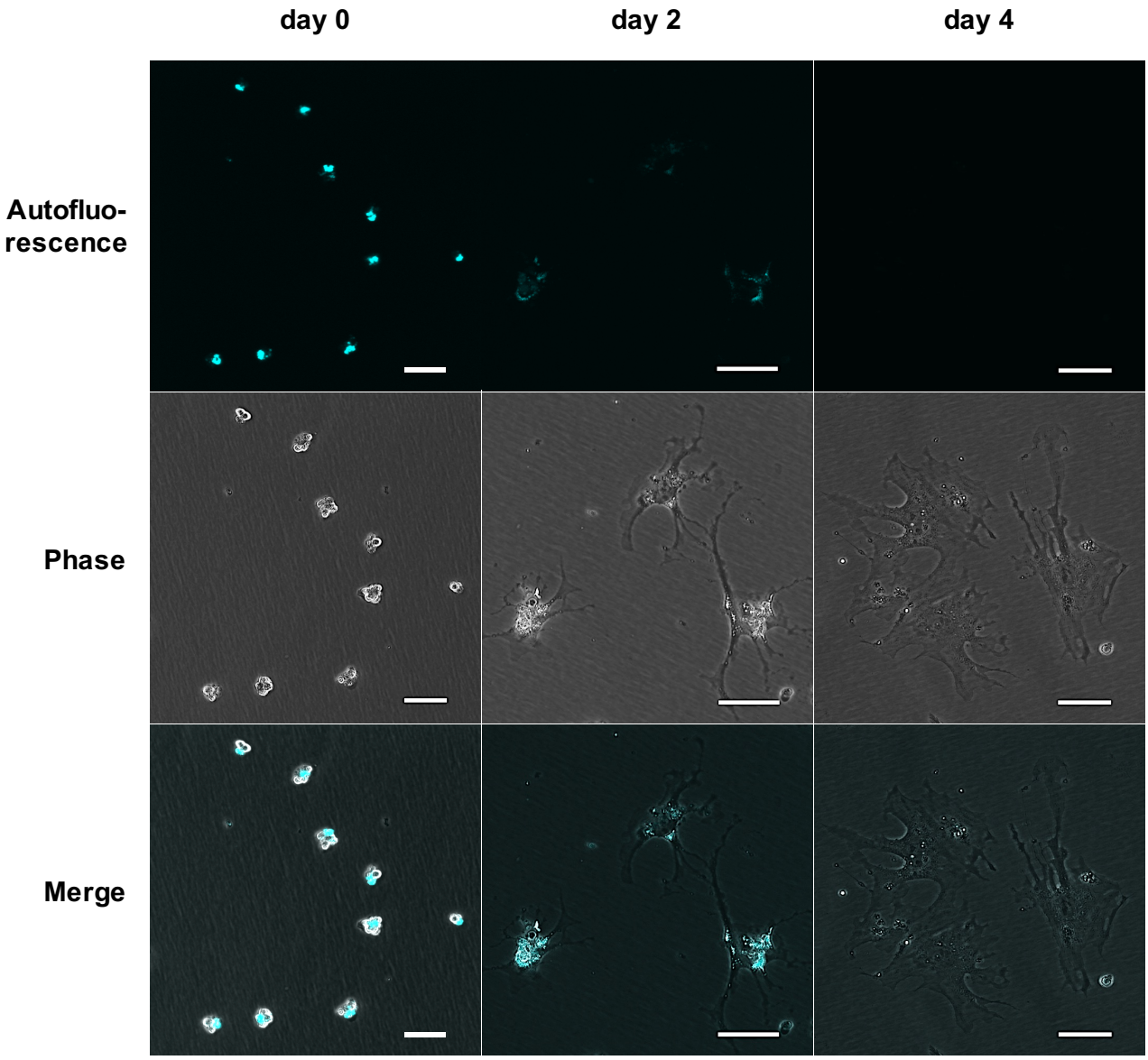

Figure 8. Primary HSCs are irregularly round shaped, and retinol-rich lipid droplets emit cyan autofluorescence by 352 nm LASER. The HSCs cultured for 2 days became extended and presented an asteroid phenotype, whereas large numbers of lipid droplets were still observed. No autofluorescence was detected after culturing HSCs for 4 days, and the cells extended further. Scale bars = 50 μm.

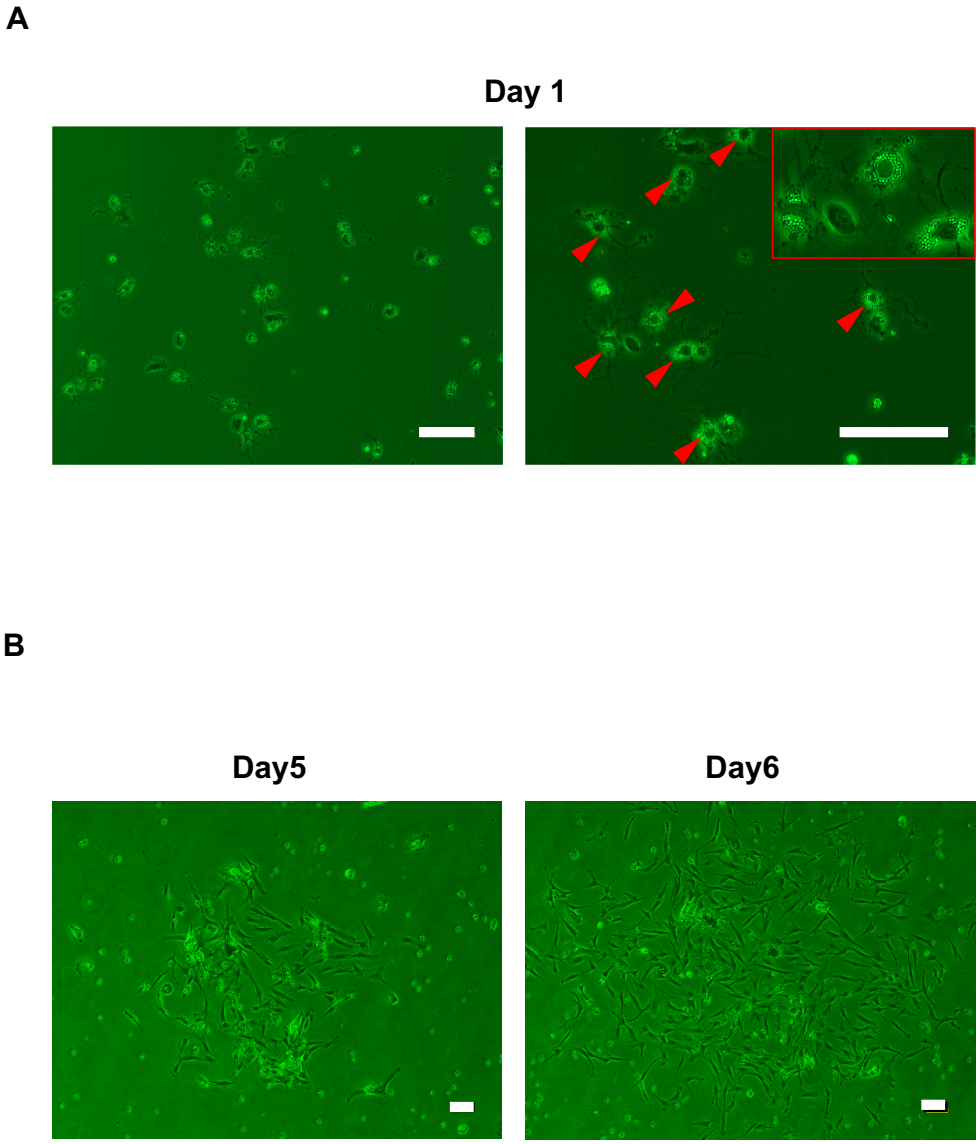

Figure 9. Morphology of sorted HSCs *in vitro*. (A) Most of the seeded HSCs present an asteroid phenotype with remaining a great quantity of lipid droplets after 1 day of culture. Arrows indicate lipid droplets and the inset at the upper right corner shows the lipid droplets close-up. Scale bars = 100 μm. (B) Sorted HSCs proliferated during culture and presented a fibroblast-like phenotype. Scale bars = 100 μm.

3 Effects of hAMSC-CM on Routinely Cultured HSCs

Next, I investigated whether hAMSC-CM inhibits the pro-fibrogenic effects of HSCs, which is a key contributor for fibrosis. After culturing HSCs with hAMSC-CM for 48 hours, immunofluorescence staining indicated that α-SMA expression in HSCs was much lower compared to HSCs cultured in SM (Fig. 10A). Consistently, qRT-PCR showed that hAMSC-CM significantly decreased *α-Sma* expression (Fig. 10B). Then, I examined the expression profile of fibrosis-related genes of HSCs. Compared to control HSCs, hAMSC-CM did not affect collagen type 1 alpha 1 (*Col1a1*) expression (Fig. 11A). On the other hand, although tissue inhibitor of metalloproteinase (*Timp*)-2 expression did not vary, hAMSC-CM significantly up-regulated the expression of metalloproteinase (*Mmp*)*-2, Mmp-9, Mmp-13*, and *Timp-1* (Fig. 11A). In addition, hAMSC-CM markedly increased the *Mmp-13/Timp-1* ratio, an index for evaluating the extracellular matrix (ECM) accumulation degree (Fearon et al., 2006) (Fig. 11B), and decreased the concentration of COL1 in culture media, detected by ELISA (Fig. 11C). Investigation of the effect of hAMSC-CM on HSC proliferation showed that hAMSC-CM reduced the gene expressions of Cyclin B1 (*Ccnb-1*) and Cyclin B2 (*Ccnb-2*); however, the reduction of *Ccnb-1* was not statistically significant (Fig. 12A). The CCK-8 proliferation assay showed that hAMSC-CM significantly inhibited HSC proliferation at 48 hours (Fig. 12B). qRT-PCR and ELISA results indicated that the effect of hAMSC-CM on HSCs was concentration dependent (Fig. 10B, 11). Fibroblast-CM increased the expression of *Mmps* and *Timp-1*, and decreased the expression of *α-Sma* and *Ccnb*, however it significantly enhanced *Col1a1* expression and suppressed *Timp-2* expression in HSCs (Fig. 13).

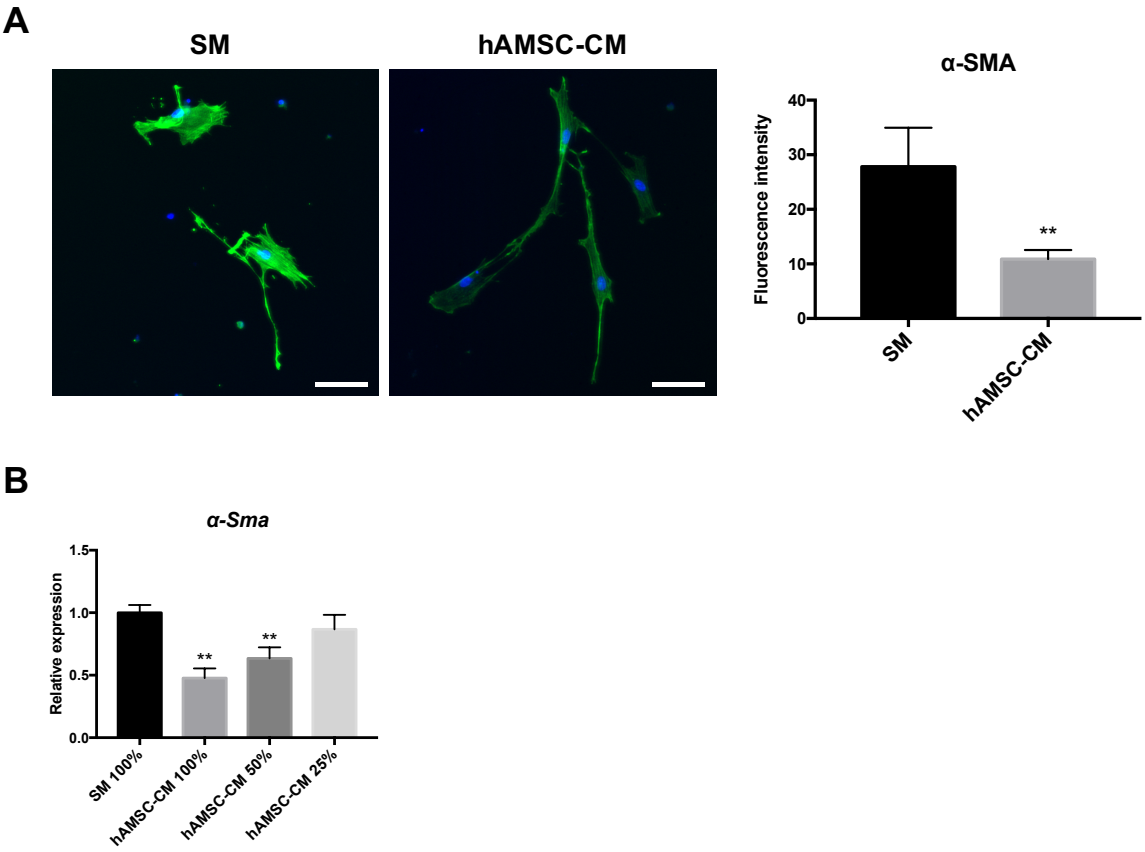

Figure 10. Effect of hAMSC-CM on primary HSC activation in routine culture. (A) Immunofluorescence staining of α-SMA (green) in HSCs cultured in SM or hAMSC-CM for 48 hours. Nuclei were stained by Hoechst 33342 (blue). Scale bars = 50 μm. Data are expressed as mean ± SD (n = 28 in the SM group and n = 24 in the hAMSC-CM group). $^{**}P < 0.01$ versus SM. (B) Expression of *α-Sma* in different concentrations of hAMSC-CM. Data are expressed as mean ± SD (n = 3). $^{**}P < 0.01$ versus SM 100%.

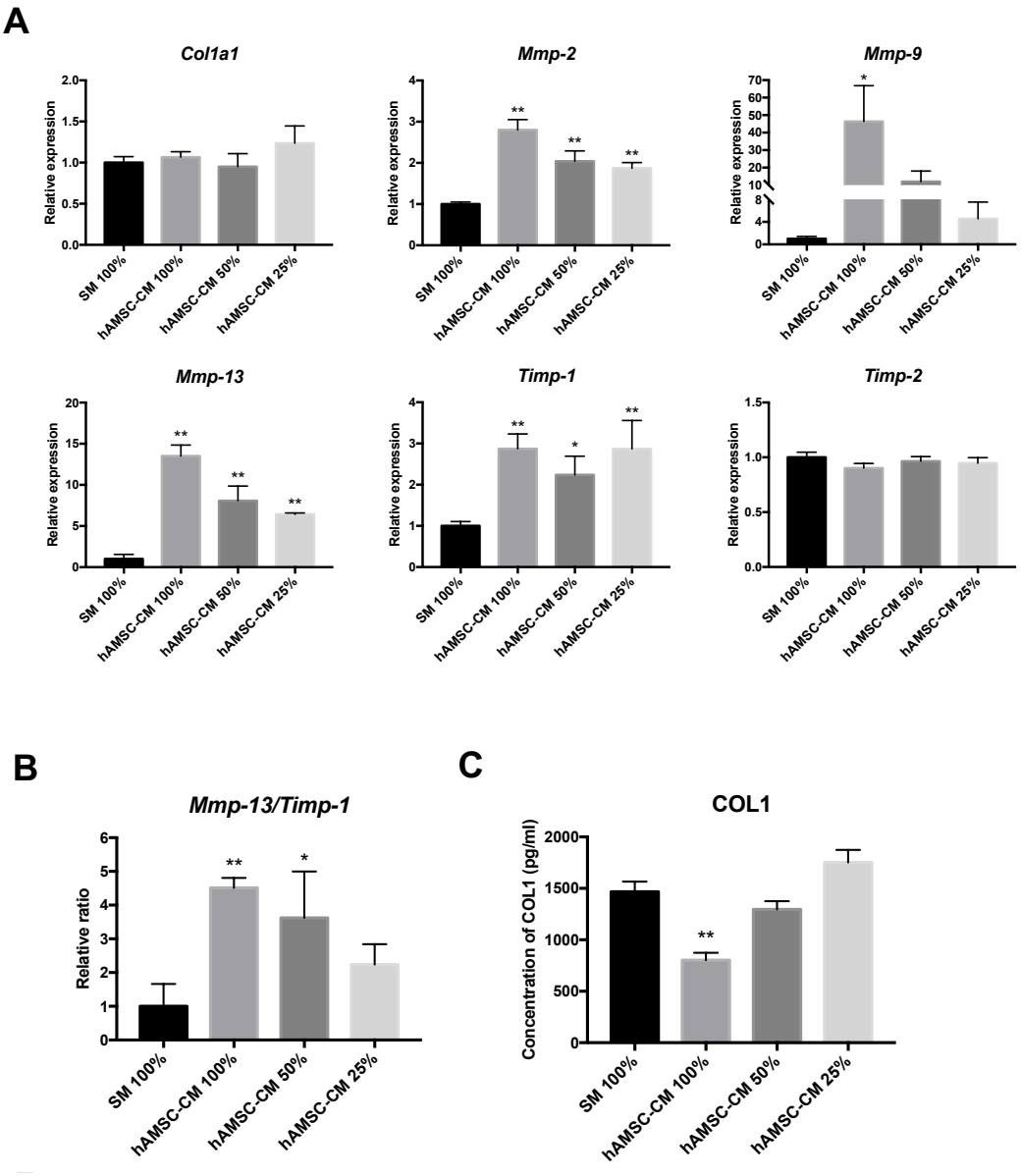

Figure 11. Effect of hAMSC-CM on ECM accumulation in routine culture. (A) ECM-related gene expression analysis of HSCs cultured in SM or different concentrations of hAMSC-CM. The data are expressed as mean ± SD (n = 3). $^{*}P <$ 0.05; $^{**}P < 0.01$ versus SM 100%. (B) Relative *Mmp-13/Timp-1* expression ratio. Data are expressed as mean ± SD (n = 3). $^{*}P < 0.05$; $^{**}P < 0.01$ versus SM 100%. (C) Expression of COL1 in culture media analyzed by ELISA. Data are expressed as mean ± SD (n = 3). $^{**}P < 0.01$ versus SM 100%.

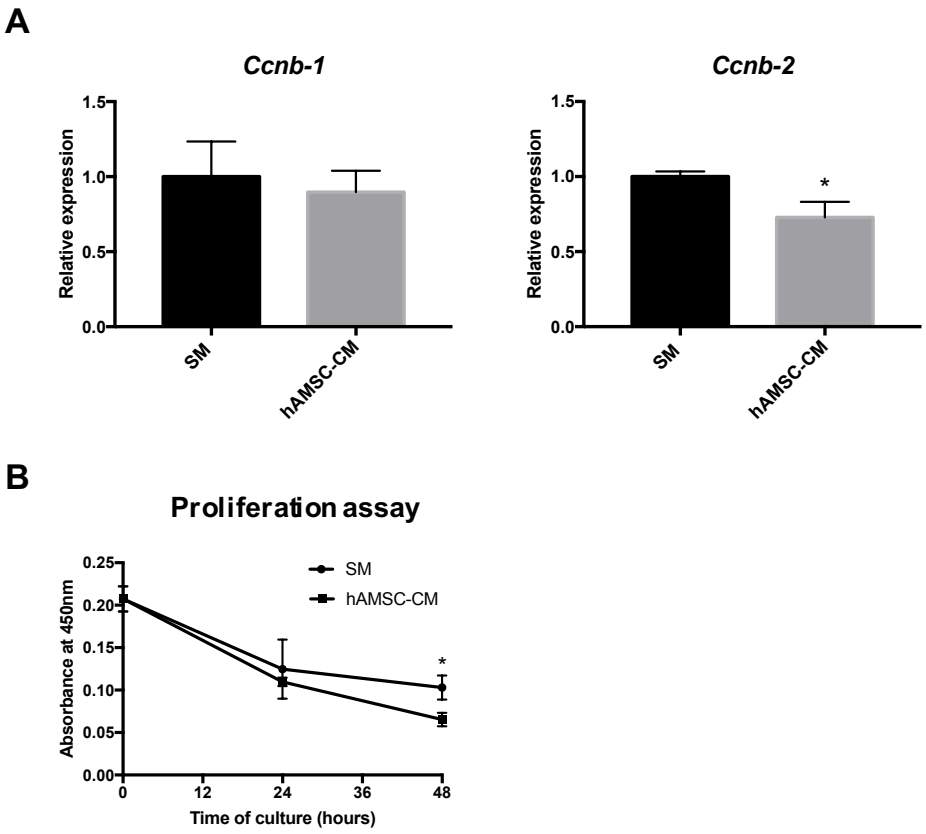

Figure 12. Effect of hAMSC-CM on primary HSC proliferation in routine culture. (A) Proliferation-related gene expression analysis for *Ccnb-1* and *Ccnb-2*. The data are expressed as mean ± SD (n = 3). $^{*}P < 0.05$ versus SM. (B) Detection of proliferation of HSCs cultured in SM or hAMSC-CM by CCK-8. The data are expressed as mean ± SD (n = 3 for each time point and culture condition). $^{*}P < 0.05$ versus SM.

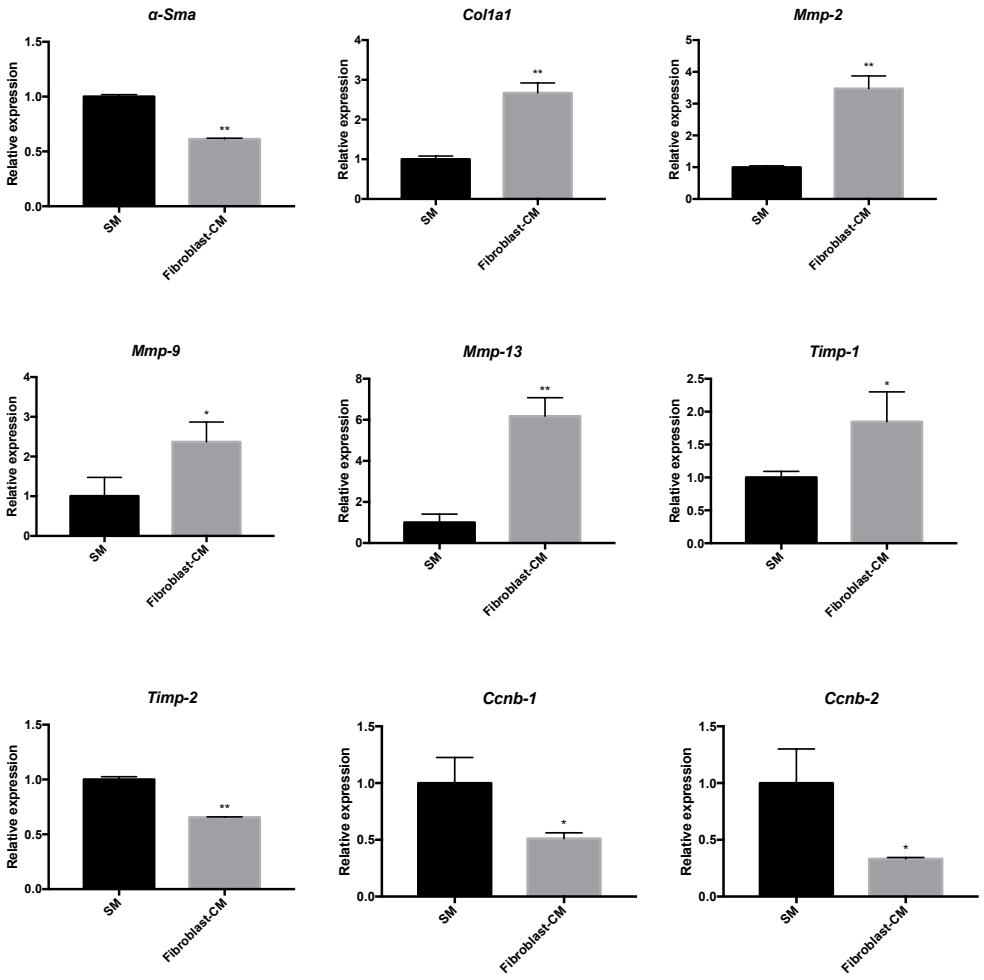

Figure 13. Gene expressions of primary HSCs cultured in SM or human skin fibroblast-CM. Data are expressed as mean ± SD (n = 3). $^{*}P < 0.05$; $^{**}P < 0.01$ versus SM.

4 Effects of hAMSC-CM on TGFβ-Treated HSCs

TGFβ is the most efficient collagen synthesis factor on HSCs (Li and Friedman, 1999); therefore, I investigated whether hAMSC-CM could reverse HSC activation and the progression of ECM accumulation after TGFβ1 stimulation. I observed that TGFβ1 up-regulated TGFβ receptor 1 (*Tgfbr1*) expression, and the increased expression of *Tgfbr1* in hAMSC-CM was greater than that in SM (Fig. 14A). At the same time, the result of TGFβ1 assay by ELISA indicated that hAMSC-CM contained a large amount of TGFβ1, whereas SM did not contain TGFβ1 (Fig. 14B). TGFβ1 significantly increased *α-Sma* expression, while hAMSC-CM inhibited the increase of TGFβ1-induced *α-Sma* expression (Fig. 15). Although hAMSC-CM did not affect *Col1a1* expression in routine culture, it significantly suppressed TGFβ1-induced up-regulation of *Col1a1* (Fig. 16A). In addition, compared to SM, hAMSC-CM significantly increased *Mmp-2*, *Mmp-9*, *Mmp-13*, and *Timp-1* expression, although there was no change in *Timp-2* expression (Fig. 16A). TGFβ1 significantly down-regulated the *Mmp-13/Timp-1* relative ratio, which was increased, however, by hAMSC-CM, even in the presence of TGFβ1 (Fig. 16B).

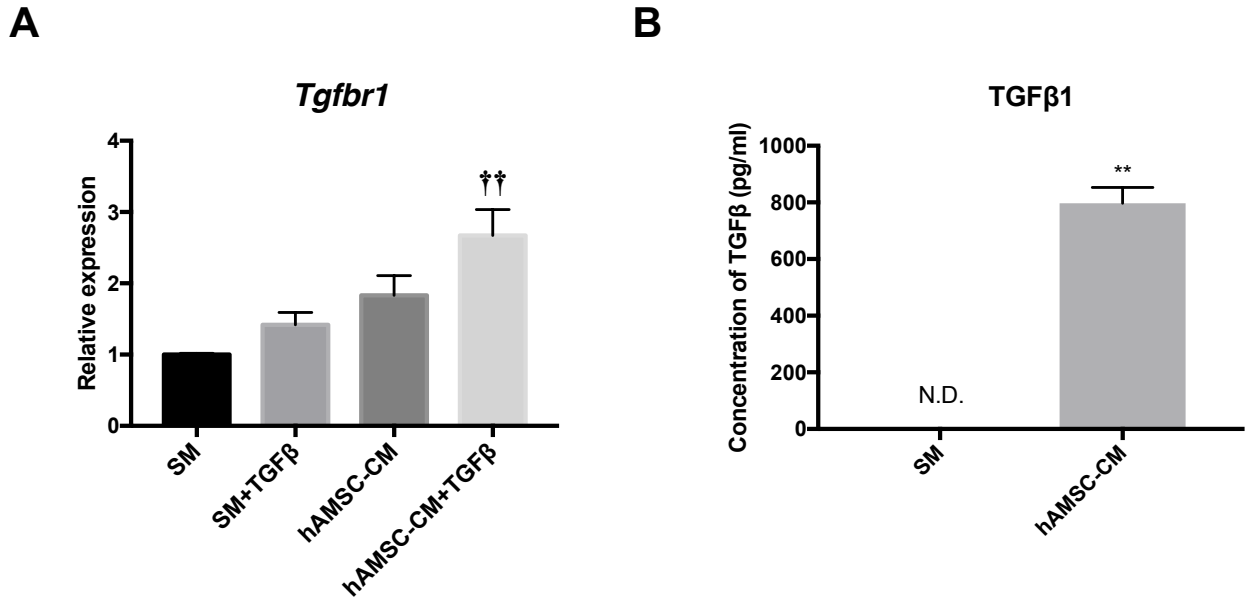

Figure 14. Effect of hAMSC-CM on TGFβ1-induced HSC activation. (A) Gene expression analysis of HSCs with or without TGFβ1 in SM or hAMSC-CM, analyzed by qRT-PCR for *Tgfbr1*. Data are expressed as mean ± SD (n = 3). $^{\dagger\dagger}P <$ 0.01 versus SM+TGFβ. (B) Content of TGFβ1 in media analyzed by ELISA. Data are expressed as mean ± SD (n = 3). $^{**}P < 0.01$ versus SM.

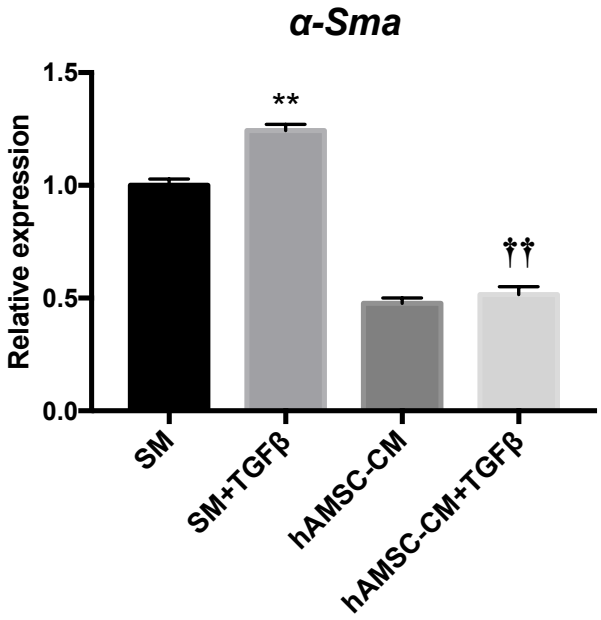

Figure 15. Effect of hAMSC-CM on TGFβ1-induced HSC activation. Gene expression analysis of HSCs with or without TGFβ1 in SM or hAMSC-CM, analyzed by qRT-PCR for *α-Sma*. Data are expressed as mean ± SD ($n = 3$). $^{**}P < 0.01$ versus SM; $^{††}P < 0.01$ versus SM+TGFβ.

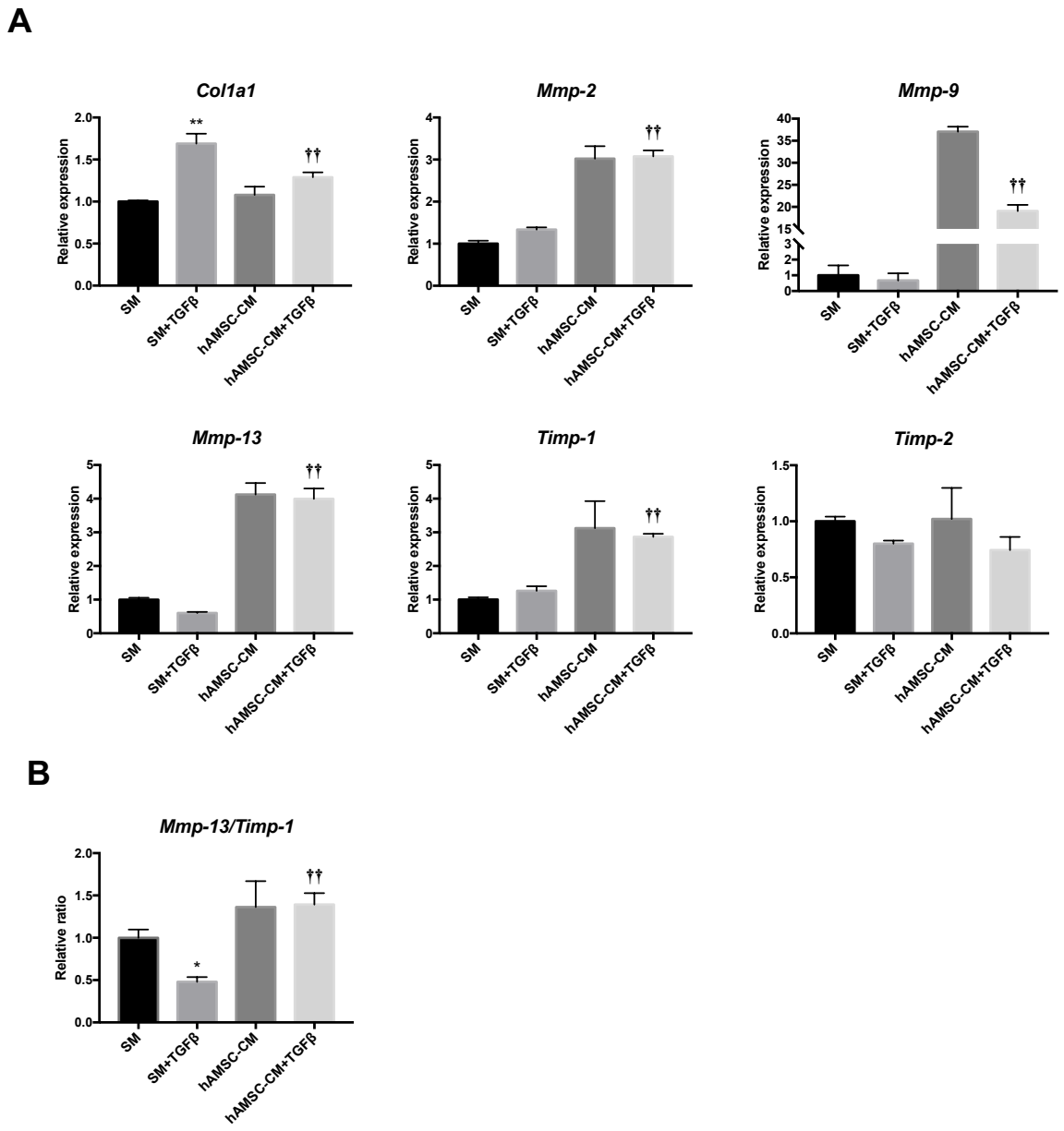

Figure 16. Effect of hAMSC-CM on TGFβ1-induced HSC activation. (A) Gene expression analysis of HSCs with or without TGFβ1 in SM or hAMSC-CM, analyzed by qRT-PCR for ECM-related genes. (D) Relative *Mmp-13/Timp-1* expression ratio. Data are expressed as mean ± SD (n = 3). $^{*}P < 0.05$; $^{**}P < 0.01$ versus SM; $^{\dagger\dagger}P < 0.01$ versus SM+TGFβ.

DISCUSSION

Previous studies have shown that hAMSC transplantation ameliorates liver fibrosis *in vivo* (Kubo et al., 2015; Zhang et al., 2011). Given that HSCs play an important role in the development of liver fibrosis (Zhang et al., 2016a), I hypothesized that hAMSCs inhibit liver fibrosis by regulating the functions of HSCs by secretory factors and I found that hAMSC-CM inhibits activation and proliferation of primary HSCs *in vitro,* and reduces the accumulation of ECM from HSCs.

Highly purified HSCs are required for mechanistic studies in liver fibrosis. Therefore, to improve their purity, I isolated HSCs with FACS-based sorting. A previous study has demonstrated that FACS can obtain unaffected, functional HSCs with high purity (Bartneck et al., 2015), and I added 7-AAD to prevent interference by nonspecific autofluorescence of dead cells and to ensure that only viable HSCs were sorted. Previous studies reported several markers for HSCs such as desmin (Yokoi et al., 1984), glial fibrillary acidic protein (GFAP) (Gard et al., 1985) and CD38 (March et al., 2007). However, the specificity of these markers is still questionable (Ballardini, 1994; March et al., 2007; Niki et al., 1996), and desmin staining in the present study showed that only 74.6 % were positive. Therefore, I chose using autofluorescence to confirm the purity of isolated HSCs instead of using those markers. In addition, cell type-specific gene expression analysis and flow cytometry analysis indicated that isolated HSCs were rarely mixed with other kinds of cells in the liver.

After sorting HSCs, I cultured them in medium with FBS and growth supplement for 48 hours to boost HSC adhesion and activation. FBS-free SM or hAMSC-CM was used in the subsequent culture because cytokines and factors present in FBS may mask the potential effects of hAMSC-CM.

HSCs are activated and proliferate rapidly in pathological conditions such as liver injury and transform into myofibroblast-like cells, which express α-SMA and secrete abundant collagen (Friedman, 2008). In this study, I demonstrated that hAMSC-CM can inhibit HSC activation, as indicated by the decreased α-SMA expression at both gene and protein levels. Excessive ECM accumulation, namely the disequilibrium of interstitial collagens, MMPs, and TIMPs, induces liver fibrosis. When HSCs are activated, large amounts of COL1, the key protein involved in liver fibrosis development, are secreted (Tsuchida and Friedman, 2017). In this study, I showed that hAMSC-CM does not influence *Col1a1* expression but has a positive effect on *Mmps* and *Timps* in routine culture of HSCs. MMP-13 is a kind of collagenase and the main protease that can degrade COL1 in a fibrotic liver (Friedman, 2008). Although *Mmp-13* up-regulation might imply that hAMSC-CM decreased the amount

of COL1, an increase in *Timp-1* made the result indistinct. TIMP-1 is an MMP inhibitor and forms tight 1:1 inhibitory complexes with MMP-13 (Iyer et al., 2007). Thus, evaluating COL1 degradation with *Mmp-13/Timp-1* is considered more objective (Fearon et al., 2006). An increase in *Mmp-13/Timp-1* by hAMSC-CM in this study suggested that hAMSC-CM may down-regulate the amount of COL1, as verified by a COL1 assay. On the other hand, studies have also reported that MMP-2 (gelatinase A) and MMP-9 (gelatinase B) bind to TIMP-2 and TIMP-1, respectively (William and Robert, 1998). Although MMP-2 and MMP-9 rarely cleave COL1, their up-regulation may also benefit COL1 degradation by blocking of TIMPs. On the basis of the above-mentioned analysis, I believe that instead of inhibiting COL1 synthesis in routine culture of HSCs, hAMSC-CM reduces ECM accumulation by promoting COL1 degradation. The mechanism by which hAMSC-CM regulate ECM accumulation is shown in Fig. 17.

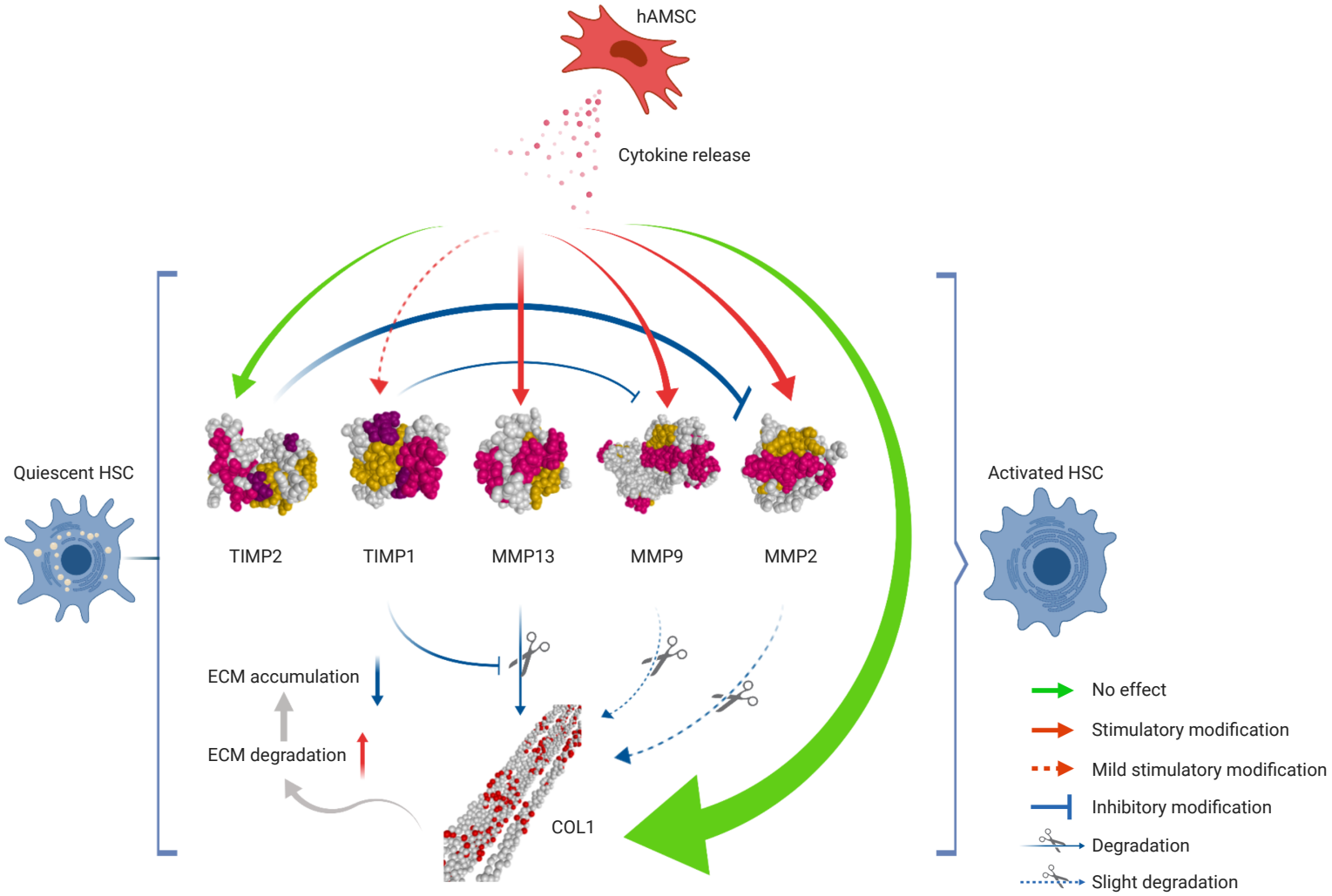

Figure 17. A putative model of hAMSC-CM regulating accumulation of ECM secreted by HSCs in routine culture.

TGFβ is the most efficient fibrogenic factor. Stimulated by TGFβ1, up-regulation of COL1 and TIMP-1 and down-regulation of MMPs lead to ECM deposition (Xu et al., 2016). In this study, hAMSC-CM reversed this pro-fibrogenic state and inhibited the increase in TGFβ1-induced *Col1a1* expression, accompanied by up-regulation of *Mmp-2*, *Mmp-9*, and *Mmp-13/Timp-1* ratio. Although studies have demonstrated that α-SMA expression does not involve the TGFβ signaling pathway (Lindert et al., 2005), the view that TGFβ intensifies α-SMA expression *in vitro* is widely accepted (Reeves and Friedman, 2002; Schuppan, 2015). In this study, I observed that TGFβ1 augments *α-Sma* expression and hAMSC-CM inhibits TGFβ1-induced HSC activation. Interestingly, compared to TGFβ1, hAMSC-CM enhances *Tgfbr1* expression, which appears to be contrary to the anti-fibrogenic effects of hAMSC-CM. In addition, I found that hAMSC-CM contains TGFβ1, and *Tgfbr1* up-regulation is most likely caused by additional exogenous TGFβ1. These results implied that hAMSC-CM exerts anti-fibrogenic functions by modifying downstream genes in the TGFβ signaling pathway or through the TGFβ-independent pathway. The possible way of hAMSC-CM in inhibiting TGFβ1-induced HSC activation is shown in Fig. 18, and further studies are required to clarify the underlying mechanism.

HSC activation is accompanied by massive cell proliferation, promoting ECM remodeling and portal resistance increase in liver fibrosis (Friedman, 2008). In this study, the CCK-8 proliferation assay indicated that hAMSC-CM reduces HSC proliferation. In addition, it down-regulates the expression of *Ccnb-1* and *Ccnb-2* which are positive cell cycle regulators strongly associated with the G2/M phase. As previous research has clarified that TGFβ1 inhibits cell cycle progression by blocking activation of cyclin-dependent kinases (Mukherjee et al., 2010), it appeared that TGFβ1 existing in hAMSC-CM is involved in suppressing HSC proliferation.

Furthermore, given that hAMSCs are likely to be contaminated with fibroblasts by using current isolation scheme and in order to investigate whether the suppressive effect on HSCs is specific to hAMCS-CM, I cultured HSCs with conditioned medium obtained from skin fibroblasts. Although fibroblast-CM increased the expression of *Mmps* and *Timp-1*, and decreased the expression of *α-Sma* and *Ccnbs*, as hAMSC-CM did, it significantly enhanced *Col1a1* expression and suppressed *Timp-2* expression in HSCs. These results suggest that hAMSCs and fibroblasts have something in common in certain functions, as same as their morphology. However, because there are few studies demonstrating the similar functions of hAMSCs and fibroblasts, their common mechanism is unclear.

In the present study, I obtained highly purified HSCs and I demonstrated the anti-activation effect of hAMSC-CM on HSCs *in vitro*. However, this study still has some

limitations. Because of the different amounts of lipid droplets in every cell, FACS may isolate only HSCs full of lipid droplets, which means that perhaps only a particular type of HSC was sorted out for experimentation. In addition, HSCs may display a significant difference *in vivo*, responding to hAMSC-CM. (De Minicis et al., 2007).

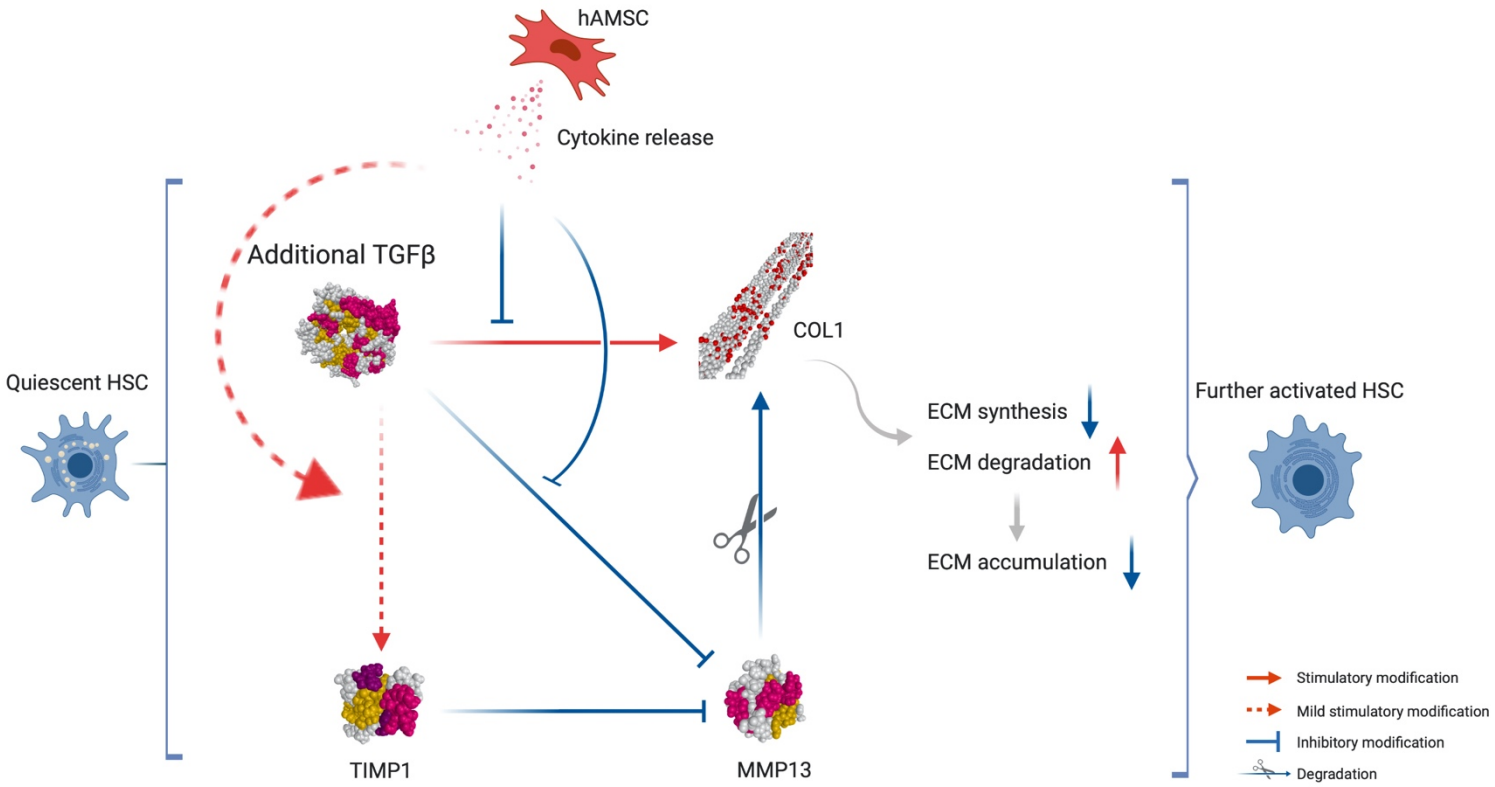

Figure 18. The possible mechanism of hAMSC-CM in regulating accumulation of ECM secreted by HSCs after TGFβ treatment.

CONCLUSION

In conclusion, the novel findings of this research are listed as below:
(i) hAMSC-CM inhibits HSC activation.
(ii) hAMSC-CM regulates ECM accumulation during HSC activation by enhancing the degradation of ECM.
(iii) hAMSC-CM suppresses HSC proliferation.

Although several clinical studies report the use of human MSCs in liver fibrosis, the application of MSCs is limited by their availability. The results of this study, while providing mechanistic evidence that hAMSCs play an inhibitory role through paracrine signaling to HSCs, proposes a new approach to the application of MSCs in therapy. Based on these evidences, the focus can be transferred from MSCs themselves to the factors or cytokines secreted by MSCs for the application of MSCs in the treatment of liver fibrosis. Obviously, adequate therapy with factors or cytokines will greatly improve safety and reduce unpredictable adverse events compared to direct application of allogeneic cells.

Future studies are required to determine the active humoral factors and their amounts in hAMSC-CM, which may provide further evidences for the clinical application of MSCs to treating liver fibrogenesis. In fact, our laboratory has begun preliminary component analysis of hAMSC-CM, and found the presence of several new components, which were greatly increased compared to the control. But further analysis, for example, the analysis of structure of new humoral factors has not yet begun for various reasons. In the future, I will expand the research of analyzing the composition of hAMSC-CM, which will be a complex and lengthy process, but worth figuring out.

ACKNOWLEDGEMENTS

Mostly, I would like to express my great appreciation to Professor SAKAMOTO NAOYA, the head of Department of Gastroenterology and Hepatology, Hokkaido University Graduate School of Medicine, for accepting me as a doctoral course student and giving me guidance.

My supervisor Associate Professor OHNISHI SHUNSUKE has been very patient to me and support my research during the past 4 years. I am very grateful to him for giving me enough freedom to plan my own research and carefully revising the manuscript of the paper over and over again, so that the paper can be accepted with only once submission. In this relaxed and friendly research atmosphere, I had a great time getting through my doctoral program.

I am obliged to Dr. HOSONO HIDETAKA for teaching me how to start a research, as well as the methods and techniques of various experiments. Thanks to his guidance, I can quickly grow from a rookie who can even not recognize the instruments' name to a researcher who can reflect and complete the experiment independently.

I also would like to thank Dr. OHARA MASATSUGU. In the first year of my doctoral course, as the only two students in the regenerative medicine group, we always discussed the progress of the research, worked together to solve problems, and helped each other. This is a very important stage in my research career, which made me realize the importance of team work very early.

I appreciated to the other faculty members of our laboratory as well. Thanks for giving me the most pertinent advice at every research conference, by which I can complete my research smoothly.

For the other staffs in the laboratory, including but not limited to the secretary, research assistants, I would like to express my sincere gratitude for the support and help in the past 4 years.

I would like to offer my special thanks to OTSUKA TOSHIMI Scholarship Foundation, thanks to the support of the foundation (No.17-s28, No.18-60, No.19-43), I can have no worries about finances and concentrate on research.

At last, I also want to express my deep appreciation to my family, and friends who have always supported and encouraged me. Especially, to my wife, who came to Japan with me and accompanied me around. This thesis is also for my unborn son, who makes my world more complete.

THE OPPOSITE OF INTEREST

The author declares no conflict of interest.

REFERENCES

Ahern, M., Hall, P., Halliday, J., Liddle, C., Olynyk, J., Ramm, G., Denk, H., Desmet, V., Geerts, A., R., B., *et al.* (1996). Hepatic stellate cell nomenclature. Hepatology *23*, 193.

Akiyama, K., Chen, C., Wang, D., Xu, X., Qu, C., Yamaza, T., Cai, T., Chen, W., Sun, L., and Shi, S. (2012). Mesenchymal-stem-cell-induced immunoregulation involves FAS-ligand-/FAS-mediated T cell apoptosis. Cell Stem Cell *10*, 544-555.

Ballardini, G. (1994). Ito cell heterogeneity:Desmin-negative Ito cells in normal rat liver. hepatology *19*.

Barlow, S., Brooke, G., Chatterjee, K., Price, G., Pelekanos, R., Rossetti, T., Doody, M., Venter, D., Pain, S., Gilshenan, K., *et al.* (2008). Comparison of human placenta- and bone marrow-derived multipotent mesenchymal stem cells. Stem Cells Dev *17*, 1095-1107.

Bartneck, M., Warzecha, K.T., Tag, C.G., Sauer-Lehnen, S., Heymann, F., Trautwein, C., Weiskirchen, R., and Tacke, F. (2015). Isolation and time lapse microscopy of highly pure hepatic stellate cells. Anal Cell Pathol (Amst) *2015*, 417023.

Bataller, R., and Brenner, D.A. (2005). Liver fibrosis. J Clin Invest *115*, 209-218.

Blomhoff, R., and Blomhoff, H.K. (2006). Overview of retinoid metabolism and function. J Neurobiol *66*, 606-630.

Brooke, G., Tong, H., Levesque, J.P., and Atkinson, K. (2008). Molecular trafficking mechanisms of multipotent mesenchymal stem cells derived from human bone marrow and placenta. Stem Cells Dev *17*, 929-940.

Cao, C., Dong, Y., and Dong, Y. (2005). Study on culture and in vitro osteogenesis of blood-derived human mesenchymal stem cells. Zhongguo Xiu Fu Chong Jian Wai Ke Za Zhi *19*, 642-647.

Caplan, A.I., and Dennis, J.E. (2006). Mesenchymal stem cells as trophic mediators. J Cell Biochem *98*, 1076-1084.

Chang, J., Hisamatsu, T., Shimamura, K., Yoneno, K., Adachi, M., Naruse, H., Igarashi, T., Higuchi, H., Matsuoka, K., Kitazume, M.T., *et al.* (2013). Activated hepatic stellate cells mediate the differentiation of macrophages. Hepatol Res *43*, 658-669.

Chen, L., Zhang, W., Zhou, Q.D., Yang, H.Q., Liang, H.F., Zhang, B.X., Long, X., and Chen, X.P. (2012). HSCs play a distinct role in different phases of oval cell-mediated liver regeneration. Cell Biochem Funct *30*, 588-596.

D'Amico, G., Garcia-Tsao, G., and Pagliaro, L. (2006). Natural history and prognostic indicators of survival in cirrhosis: a systematic review of 118 studies. J Hepatol *44*, 217-231.

De Minicis, S., Seki, E., Uchinami, H., Kluwe, J., Zhang, Y., Brenner, D.A., and Schwabe, R.F. (2007). Gene expression profiles during hepatic stellate cell activation in culture and in vivo. Gastroenterology *132*, 1937-1946.

Dominici, M., Le Blanc, K., Mueller, I., Slaper-Cortenbach, I., Marini, F., Krause, D., Deans, R., Keating, A., Prockop, D., and Horwitz, E. (2006). Minimal criteria for defining multipotent mesenchymal stromal cells. The International Society for Cellular Therapy position statement. Cytotherapy *8*, 315-317.

Fearon, U., Mullan, R., Markham, T., Connolly, M., Sullivan, S., Poole, A.R., FitzGerald, O., Bresnihan, B., and Veale, D.J. (2006). Oncostatin M induces angiogenesis and cartilage degradation in rheumatoid arthritis synovial tissue and human cartilage cocultures. Arthritis Rheum *54*, 3152-3162.

Fraser, J.K., Wulur, I., Alfonso, Z., and Hedrick, M.H. (2006). Fat tissue: an underappreciated source of stem cells for biotechnology. Trends Biotechnol *24*, 150-154.

Friedenstein, A.J. (1976). Precursor cells of mechanocytes. Int Rev Cytol *47*, 327-359.

Friedenstein, A.J., Chailakhyan, R.K., and Gerasimov, U.V. (1987). Bone marrow osteogenic stem cells: in vitro cultivation and transplantation in diffusion chambers. Cell Tissue Kinet *20*, 263-272.

Friedman, S.L. (2008). Hepatic stellate cells: protean, multifunctional, and enigmatic cells of the liver. Physiol Rev *88*, 125-172.

Gard, A.L., White, F.P., and Dutton, G.R. (1985). Extra-neural glial fibrillary acidic protein (GFAP) immunoreactivity in perisinusoidal stellate cells of rat liver. J Neuroimmunol *8*, 359-375.

Geerts, A. (2001). History, heterogeneity, developmental biology, and functions of quiescent hepatic stellate cells. Semin Liver Dis *21*, 311-335.

Geerts, A., Niki, T., Hellemans, K., De Craemer, D., Van Den Berg, K., Lazou, J.M., Stange, G., Van De Winkel, M., and De Bleser, P. (1998). Purification of rat hepatic stellate cells by side scatter-activated cell sorting. Hepatology *27*, 590-598.

Gressner, A.M., Krull, N., and Bachem, M.G. (1994). Regulation of proteoglycan expression in fibrotic liver and cultured fat-storing cells. Pathol Res Pract *190*, 864-882.

Griffiths, M.J., Bonnet, D., and Janes, S.M. (2005). Stem cells of the alveolar epithelium. Lancet *366*, 249-260.

Hass, R., Kasper, C., Bohm, S., and Jacobs, R. (2011). Different populations and sources of human mesenchymal stem cells (MSC): A comparison of adult and neonatal tissue-derived MSC. Cell Commun Signal *9*, 12.

Hellerbrand, C. (2013). Hepatic stellate cells--the pericytes in the liver. Pflugers Arch *465*, 775-778.
In 't Anker, P.S., Scherjon, S.A., Kleijburg-van der Keur, C., de Groot-Swings, G.M., Claas, F.H., Fibbe, W.E., and Kanhai, H.H. (2004). Isolation of mesenchymal stem cells of fetal or maternal origin from human placenta. Stem Cells *22*, 1338-1345.
Ito, T., and Nemoto, M. (1952). Kupfer's cells and fat storing cells in the capillary wall of human liver. Okajimas Folia Anat Jpn *24*, 243-258.
Iyer, S., Wei, S., Brew, K., and Acharya, K.R. (2007). Crystal structure of the catalytic domain of matrix metalloproteinase-1 in complex with the inhibitory domain of tissue inhibitor of metalloproteinase-1. J Biol Chem *282*, 364-371.
Karp, J.M., and Leng Teo, G.S. (2009). Mesenchymal stem cell homing: the devil is in the details. Cell Stem Cell *4*, 206-216.
Kia, R., Sison, R.L., Heslop, J., Kitteringham, N.R., Hanley, N., Mills, J.S., Park, B.K., and Goldring, C.E. (2013). Stem cell-derived hepatocytes as a predictive model for drug-induced liver injury: are we there yet? Br J Clin Pharmacol *75*, 885-896.
Kubo, K., Ohnishi, S., Hosono, H., Fukai, M., Kameya, A., Higashi, R., Yamada, T., Onishi, R., Yamahara, K., Takeda, H.*, et al.* (2015). Human Amnion-Derived Mesenchymal Stem Cell Transplantation Ameliorates Liver Fibrosis in Rats. Transplant Direct *1*, e16.
Kundrotas, G. (2012). Surface markers distinguishing mesenchymal stem cells from broblasts. ACTA MEDICA LITUANICA *19*, 75-79.
Lee, U.E., and Friedman, S.L. (2011). Mechanisms of hepatic fibrogenesis. Best Pract Res Clin Gastroenterol *25*, 195-206.
Lee, Y.A., Wallace, M.C., and Friedman, S.L. (2015). Pathobiology of liver fibrosis: a translational success story. Gut *64*, 830-841.
Li, D., and Friedman, S.L. (1999). Liver fibrogenesis and the role of hepatic stellate cells: new insights and prospects for therapy. J Gastroenterol Hepatol *14*, 618-633.
Lindert, S., Wickert, L., Sawitza, I., Wiercinska, E., Gressner, A.M., Dooley, S., and Breitkopf, K. (2005). Transdifferentiation-dependent expression of alpha-SMA in hepatic stellate cells does not involve TGF-beta pathways leading to coinduction of collagen type I and thrombospondin-2. Matrix Biol *24*, 198-207.
Liras, A. (2010). Future research and therapeutic applications of human stem cells: general, regulatory, and bioethical aspects. J Transl Med *8*, 131.
Liu, W., Hou, Y., Chen, H., Wei, H., Lin, W., Li, J., Zhang, M., He, F., and Jiang, Y. (2011). Sample preparation method for isolation of single-cell types from mouse liver for proteomic studies. Proteomics *11*, 3556-3564.

Lozano, R., Naghavi, M., Foreman, K., Lim, S., Shibuya, K., Aboyans, V., Abraham, J., Adair, T., Aggarwal, R., Ahn, S.Y., *et al.* (2012). Global and regional mortality from 235 causes of death for 20 age groups in 1990 and 2010: a systematic analysis for the Global Burden of Disease Study 2010. Lancet *380*, 2095-2128.

Lv, F.J., Tuan, R.S., Cheung, K.M., and Leung, V.Y. (2014). Concise review: the surface markers and identity of human mesenchymal stem cells. Stem Cells *32*, 1408-1419.

March, S., Graupera, M., Rosa Sarrias, M., Lozano, F., Pizcueta, P., Bosch, J., and Engel, P. (2007). Identification and functional characterization of the hepatic stellate cell CD38 cell surface molecule. Am J Pathol *170*, 176-187.

Marra, F. (2002). Chemokines in liver inflammation and fibrosis. Front Biosci *7*, d1899-1914.

Mederacke, I., Dapito, D.H., Affo, S., Uchinami, H., and Schwabe, R.F. (2015). High-yield and high-purity isolation of hepatic stellate cells from normal and fibrotic mouse livers. Nat Protoc *10*, 305-315.

Meirelles Lda, S., Fontes, A.M., Covas, D.T., and Caplan, A.I. (2009). Mechanisms involved in the therapeutic properties of mesenchymal stem cells. Cytokine Growth Factor Rev *20*, 419-427.

Mormone, E., George, J., and Nieto, N. (2011). Molecular pathogenesis of hepatic fibrosis and current therapeutic approaches. Chem Biol Interact *193*, 225-231.

Muhlbauer, M., Fleck, M., Schutz, C., Weiss, T., Froh, M., Blank, C., Scholmerich, J., and Hellerbrand, C. (2006). PD-L1 is induced in hepatocytes by viral infection and by interferon-alpha and -gamma and mediates T cell apoptosis. J Hepatol *45*, 520-528.

Mukherjee, P., Winter, S.L., and Alexandrow, M.G. (2010). Cell cycle arrest by transforming growth factor beta1 near G1/S is mediated by acute abrogation of prereplication complex activation involving an Rb-MCM interaction. Mol Cell Biol *30*, 845-856.

Niki, T., De Bleser, P.J., Xu, G., Van Den Berg, K., Wisse, E., and Geerts, A. (1996). Comparison of glial fibrillary acidic protein and desmin staining in normal and CCl4-induced fibrotic rat livers. Hepatology *23*, 1538-1545.

Osawa, Y., Hoshi, M., Yasuda, I., Saibara, T., Moriwaki, H., and Kozawa, O. (2013). Tumor necrosis factor-alpha promotes cholestasis-induced liver fibrosis in the mouse through tissue inhibitor of metalloproteinase-1 production in hepatic stellate cells. PLoS One *8*, e65251.

Parolini, O., Alviano, F., Bagnara, G.P., Bilic, G., Buhring, H.J., Evangelista, M., Hennerbichler, S., Liu, B., Magatti, M., Mao, N., *et al.* (2008). Concise review: isolation and characterization of cells from human term placenta: outcome of the first international Workshop on Placenta Derived Stem Cells. Stem Cells *26*, 300-311.

Reeves, H.L., and Friedman, S.L. (2002). Activation of hepatic stellate cells--a key issue in liver fibrosis. Front Biosci *7*, d808-826.
Reynaert, H., Urbain, D., and Geerts, A. (2008). Regulation of sinusoidal perfusion in portal hypertension. Anat Rec (Hoboken) *291*, 693-698.
Rockey, D.C. (2013). Translating an understanding of the pathogenesis of hepatic fibrosis to novel therapies. Clin Gastroenterol Hepatol *11*, 224-231 e221-225.
Schuppan, D. (2015). Liver fibrosis: Common mechanisms and antifibrotic therapies. Clin Res Hepatol Gastroenterol *39 Suppl 1*, S51-59.
Schuppan, D., and Afdhal, N.H. (2008). Liver cirrhosis. Lancet *371*, 838-851.
Shu, S.N., Wei, L., Wang, J.H., Zhan, Y.T., Chen, H.S., and Wang, Y. (2004). Hepatic differentiation capability of rat bone marrow-derived mesenchymal stem cells and hematopoietic stem cells. World J Gastroenterol *10*, 2818-2822.
Si-Tayeb, K., Noto, F.K., Nagaoka, M., Li, J., Battle, M.A., Duris, C., North, P.E., Dalton, S., and Duncan, S.A. (2010). Highly efficient generation of human hepatocyte-like cells from induced pluripotent stem cells. Hepatology *51*, 297-305.
Stanko, P., Kaiserova, K., Altanerova, V., and Altaner, C. (2014). Comparison of human mesenchymal stem cells derived from dental pulp, bone marrow, adipose tissue, and umbilical cord tissue by gene expression. Biomed Pap Med Fac Univ Palacky Olomouc Czech Repub *158*, 373-377.
Su, Y.H., Shu, K.H., Hu, C., Cheng, C.H., Wu, M.J., Yu, T.M., Chuang, Y.W., Huang, S.T., and Chen, C.H. (2012). Hepatic stellate cells attenuate the immune response in renal transplant recipients with chronic hepatitis. Transplant Proc *44*, 725-729.
Sun, L., Akiyama, K., Zhang, H., Yamaza, T., Hou, Y., Zhao, S., Xu, T., Le, A., and Shi, S. (2009). Mesenchymal stem cell transplantation reverses multiorgan dysfunction in systemic lupus erythematosus mice and humans. Stem Cells *27*, 1421-1432.
Tacke, F., and Weiskirchen, R. (2012). Update on hepatic stellate cells: pathogenic role in liver fibrosis and novel isolation techniques. Expert Rev Gastroenterol Hepatol *6*, 67-80.
Trautwein, C., Friedman, S.L., Schuppan, D., and Pinzani, M. (2015). Hepatic fibrosis: Concept to treatment. J Hepatol *62*, S15-24.
Tsochatzis, E.A., Bosch, J., and Burroughs, A.K. (2014). Liver cirrhosis. Lancet *383*, 1749-1761.
Tsuchida, T., and Friedman, S.L. (2017). Mechanisms of hepatic stellate cell activation. Nat Rev Gastroenterol Hepatol *14*, 397-411.
Uccelli, A., Moretta, L., and Pistoia, V. (2008). Mesenchymal stem cells in health and disease. Nat Rev Immunol *8*, 726-736.

Ward, A., Klassen, D.K., Franz, K.M., Giwa, S., and Lewis, J.K. (2018). Social, economic, and policy implications of organ preservation advances. Curr Opin Organ Transplant *23*, 336-346.
Wei, X., Yang, X., Han, Z.P., Qu, F.F., Shao, L., and Shi, Y.F. (2013). Mesenchymal stem cells: a new trend for cell therapy. Acta Pharmacol Sin *34*, 747-754.
William, C.P., and Robert, P.M. (1998). Matrix Metalloprpteinases (United States of America: Academic Press-Elsevier Science).
Xu, F., Liu, C., Zhou, D., and Zhang, L. (2016). TGF-beta/SMAD Pathway and Its Regulation in Hepatic Fibrosis. J Histochem Cytochem *64*, 157-167.
Yokoi, Y., Namihisa, T., Kuroda, H., Komatsu, I., Miyazaki, A., Watanabe, S., and Usui, K. (1984). Immunocytochemical detection of desmin in fat-storing cells (Ito cells). Hepatology *4*, 709-714.
Zhang, C.Y., Yuan, W.G., He, P., Lei, J.H., and Wang, C.X. (2016a). Liver fibrosis and hepatic stellate cells: Etiology, pathological hallmarks and therapeutic targets. World J Gastroenterol *22*, 10512-10522.
Zhang, D., Jiang, M., and Miao, D. (2011). Transplanted human amniotic membrane-derived mesenchymal stem cells ameliorate carbon tetrachloride-induced liver cirrhosis in mouse. PLoS One *6*, e16789.
Zhang, Q., Qu, Y., Li, Z., Zhang, Q., Xu, M., Cai, X., Li, F., and Lu, L. (2016b). Isolation and Culture of Single Cell Types from Rat Liver. Cells Tissues Organs *201*, 253-267.
Zhang, Z., and Wang, F.S. (2013). Stem cell therapies for liver failure and cirrhosis. J Hepatol *59*, 183-185.